2014

HcpR of Porphyromonas gingivalis utilizes heme to bind NO

Benjamin Belvin
Virginia Commonwealth University

HcpR of *Porphyromonas gingivalis* utilizes heme to bind nitric oxide

A thesis submitted in partial fulfillment for the requirements for the degree of Masters of Science in Biochemistry at Virginia Commonwealth University.

By
Benjamin Ross Belvin
Bachelor of Science (Biochemistry), Virginia Tech, Blacksburg, Virginia
May 2012

Director: **JANINA P. LEWIS**, Ph.D., Associate Professor

The Philips Institute for Oral Health Research
School of Dentistry, Virginia Commonwealth University

Virginia Commonwealth University

Richmond, Virginia

April 2014

Acknowledgements

First and foremost I would like to thank my project advisor, Dr. Janina P. Lewis. She has been an outstanding mentor and I am extremely grateful for the opportunity she has afforded me. Without her support, knowledge, and guidance none of this would have been possible. I owe her my sincerest gratitude for inviting me into her lab and giving me all the necessities, tools, and training I needed to succeed.

I would like to thank the members of my committee: Dr. Carlos Escalante for his advice, input, and access to his lab, and Dr. Jessica Bell for her guidance and expertise on the direction of my project.

I would also like to acknowledge Dr. Darrell Peterson for his help, insight, and advice on many aspects of my project. Dr. Faik Musayev for his expertise on structure and crystallography. Dr. James Terner, without whom a large part of this project would not have been possible. His expertise and knowledge on heme proteins and Raman spectroscopy has been indispensable.

I would be amiss if I did not thank every member of the Lewis lab. DJ Kang, who trained and taught me from the onset. Our lab technician Nicai Zollar, a great addition to the lab, and has helped me on countless number of occasions. My fellow students Romana Cvitkovic, Holly Dwyer, Dado Kim (honorary lab member), Soheil Rostami, Kat Sinclair, David Smith, and Chris Wunsch. All of whom provided many hours of entertainment and made being in the lab a lot more enjoyable.

A special thanks to all of my colleagues in the Wood building and Phillips Institute.

Last but definitely not least I would like to thank my parents, David and Jackie Belvin and sister, Emma. I am indebted to my family for all they have done for me. They have supported me in every endeavor, provided moral and emotional support, as well as encouragement and prayer. Without them none of this would have been remotely possible. I love you guys!

Table of Contents

Acknowledgement - ..... **ii**

List of Tables ..... **vi**

List of Figures ..... **vii**

Abstract ..... **ix**

1. Background Significance **1**

1.1 Periodontal Disease 1

1.2 *Porphyromonas gingivalis* 3

1.3 Heme-Proteins 7

1.4 NO and its role in Biology 10

1.5 Transcription factors and the regulation of stress responses in bacterial cells 15

1.6 Nitrosative stress and *Porphyromonas gingivalis* 19

1. Hypothesis and Aims **22**

2.1 - Hypothesis 22

2.2 – Aims 22

3. Materials and Methods **24**

3.1 Bioinformatics 24

3.2 Cloning and Expression 24

3.3 Purification of HcpR 28

3.4 Native gel of HcpR electrophoresis 29

3.5 Analytical centrifugation 30

3.6 TMBZ assay for heme 30

3.7 UV-Vis studies 30

3.8 Fluorescence binding assays 31

3.9 CD studies 31

3.10 Resonance Raman Spectroscopy 32

3.11 Small Angle X-Ray scattering (SAXS) data acquisition, analysis, and modeling 33

3.12 *hcp* promoter studies 33

3.13 Crystal screening 34

4. Results **37**

4.1 Bioinformatics results 37

4.2 Expression and purification of HcpR 44

4.3 Molecular weight calculation 45
4.4 Analysis of heme binding 48
4.5 Analysis of NO binding 58
4.6 HcpR structural analysis with SAXS 62
4.7 Activation of at Hcp promoter in *E. coli.* 73
4.8 Crystallization of HcpR 77
5. Discussion 80
5.1 Conclusion 87
6. Bibliography 88

List of Tables

Table 1 – Primers used in this study 29

Table 2 – Vectors used in this study 31

Table 3 – Measurement of Heme to HcpR binding through intrinsic HcpR fluorescence quenching ..77

Table 4 – Parameters from SAXS data 88

List of Figures

Figure 1 – Reactive nitrogen and reactive oxygen species 12
Figure 2 – The bacterial inorganic nitrogen cycle 13
Figure 3 - General scheme of inter-protein signal transition of a heme sensor 18
Figure 4 - Schematic overview of promoter studies 25
Figure 5 – Constructs used in promoter studies 36
Figure 6 – Superimposed structures of HcpR and DNR 39
Figure 7 – Dimeric homology model of HcpR 40
Figure 8 – Domains of HcpR homology model 41
Figure 9 – Hydrophobic residues in the heme binding pocket 42
Figure 10 – InterProscan 4 results 43
Figure 11 – SDS-PAGE gel of Purified HcpR 45
Figure 12 – Native gel of pET30-*hcpr* purified protein 47
Figure 13 – Sedimentation velocity experiment of tag-less HcpR 48
Figure 14 – TMBZ assay for heme binding of HcpR 51
Figure 15 – CD spectra of apo- and heme-HcpR 52
Figure 16 – Heme time scan titration of HcpR 53
Figure 17 - Affinity of HcpR for heme under aerobic conditions 55
Figure 18 – UV-Vis spectrum of heme binding under anaerobic conditions 56
Figure 19 – Affinity of HcpR to heme – fluorescence generated titration binding curve. 58
Figure 20- Anaerobic UV-Vis spectrum of HcpR – with NO 60
Figure 21 – Resonance Raman spectrum of HcpR 61
Figure 22 – SAXS scattering profile and Guinier plot for apo-HcpR 65
Figure 23 – SAXS scattering profile and Gunier plot for heme-HcpR 66
Figure 24 – SAXS scattering profile and Gunier plot for DNA-HcpR 67
Figure 25 – SAXS Kratky plots 68
Figure 26 – SAXS distance distribution functions (P(r)) plots 69
Figure 27 – Comparison to theoretical scattering profiles 70
Figure 28 – *ab initio* model of apo-HcpR 71
Figure 29 – *ab initio* model of heme-HcpR 72
Figure 30 – *ab initio* model of DNA-HcpR 73
Figure 31 – NO and Nitrite stimulated activation of the *hcp* promoter by HcpR in *E. coli.* 75

Figure 32 – Basal level expression of fluorescent reporter gene for different constructs 76
Figure 33 – HcpR crystals from screening 78
Figure 34 – HcpR crystal diffraction pattern 79

Abstract

HCPR OF *PORPHYROMONAS GINGIVALIS* UTILIZES HEME TO BIND NO

By: B. Ross Belvin, B.S.

A thesis submitted in partial fulfillment of the requirements for the degree of Master of Science at Virginia Commonwealth University.

Virginia Commonwealth University, 2014

Major Director: Janina P. Lewis, Ph.D., Philips Institute for Oral Health Research

The obligate anaerobe *Porphyromonas gingivalis* is the etiological agent responsible for periodontal disease. It must withstand high levels of reactive nitrogen species in the oral cavity generated by the host and other oral flora. The mechanisms allowing for protection against such stress remain poorly understand. HcpR is an FNR-CRP family regulator that has been implicated in regulation of the nitrosative stress response. In this study we characterize the biochemical properties of HcpR. It is a homo-dimer that is composed of 3 domains – a heme-binding domain, dimerization helix, and a DNA-binding domain. Our studies show that HcpR binds the heme cofactor. UV-Vis and Raman spectroscopy reveal that the bound heme is capable of binding the diatomic gas molecule Nitric Oxide (NO)-a source of nitrosative stress. Binding of NO causes a change in the oxidation state of the iron. SAXS reveals the protein bears a structural resemblance to homology models generated from an ortholog. Promoterr studies reveal that mechanisms *P. gingivalis*-HcpR uses to modulate expression are novel and different than those found in *E. coli* and *P. aeruginosa*.

Chapter 1 – Background Significance

1.1 Periodontal Disease

The wet and warm environment of the mouth is an excellent habitat for microbes to live. The oral cavity is home to over 700 different species of bacterium, most of which are commensal (Hasegawa, Mans et al. 2007). The mouth provides a variety of surfaces for bacterial colonization; most are freely exposed however there are a number of protected “pockets” on the occlusal surfaces of teeth, gaps between teeth, and on the gingival margin. The accumulation of a bacterial biofilm on teeth is termed “dental plaque” and there is an estimated 10^{11} organisms per gram of plaque (Gibbons, Houte 1975, Darveau, Tanner et al. 1997).

Under normal homeostatic conditions, there is a balance between the host immune response and the normal oral flora. This equilibrium is not indiscriminate but a highly evolved process: the dental bacteria have adapted to living and growing in the selective conditions of the mouth and the host immune response limits growth via a combination of innate and adaptive immune responses. Under certain conditions, such as immune deficiency, oral bacterium can trigger the inflammatory response. When the balance between the oral flora and the host response is upset the oral homeostasis is disrupted, the loss of this homeostatic interaction leads to the development of periodontal diseases (Darveau, Tanner et al. 1997). *Porphyromonas gingivalis,* a bacterium that is commensal in small concentrations in health individuals, is implicated as the prime etiological agent and is largely responsible for the inflammatory response seen in patients with periodontitis.

Periodontitis is defined as the presence of gingival inflammation at sites where there has been a pathological detachment of collagen fibers from the cementum and loss of the junctional epithelium. Put simply, it is an inflammatory disease that affects the tissues that surround and support the teeth. It is characterized by the loss of alveolar bone around the teeth which can lead to loosening and eventual loss of teeth if left untreated. Bacterial plaque occupies the periodontal pockets and attaches to the root surfaces. Coupled with the production of enzymes and toxins, bacteria penetrate the epithelium which leads to initiation and sustainment of the inflammatory response (Saglie, Newman et al. 1982). Periodontitis is diagnosed via clinical examination of the tissue surrounding the teeth and an X-ray radiographic examination to evaluate the bone loss surrounding the teeth (Savage, Eaton et al. 2009).

It is estimated that 47.2% of adults aged 30 years and older have some form of periodontal disease: 8.7% mild, 30.0% moderate, and 8.5% severe. The risk of obtaining a periodontal disease increased with age: it is estimated that 70.1% of adults 65 years and older have some form of periodontal disease (Eke, Dye et al. 2012). Furthermore, it has been shown that patients with immunodeficiency are at a much higher risk for chronic periodontal diseases (Klein, Harris et al. 1984). The side effects of a chronic periodontal disease have shown to increase the risk of stroke (Buhlin, Mäntylä et al. 2011) and heart disease (D'Aiuto, Parkar et al. 2006, Beck, Garcia et al. 1996).

1.2 *Porphyromonas gingivalis*

Porphyromonas gingivalis is a rod-shaped, non-motile, Gram-negative anaerobic, pathogenic bacterium that forms black colonies on blood agar plates. *P. gingivalis* is the primary etiologic agent of periodontal disease (Slots, Bragd et al. 1986). Although it is found predominantly in the mouth, *P. gingivalis* and other members of the phylum Bacteroidetes can also be found in the GI tract, respiratory tract, and colon where they can serve as opportunistic pathogens. *P. gingivalis* does not use sugars as a source of energy, instead it metabolizes peptides and other nitrogenous compounds as a source of energy, and thus it is an asaccharolytic bacterium that is dependent on its proteolytic properties for energy. In the process it generates a micro-environment abundant in ammonia and other important nitrogenous metabolic byproducts (Boutrin, Wang et al. 2012). *P. gingivalis* exhibits similarity to other medically relevant bacterium such as *Bacteroides fragilis, Prevotella intermedia* and *Tannerella forsythia* making it an excellent model bacterium to study.

Porphyromonas gingivalis is theorized to be “keystone pathogen”. The keystone pathogen hypothesis states that certain low-abundance microbial pathogens can orchestrate inflammatory disease by remodeling a normally benign microbiota into a dysbiotic one (Hajishengallis, Darveau et al. 2012). Recent studies have shown that *P. gingivalis* has evolved methods to evade components of the host immune system. Instead of acting directly as the sole pro-inflammatory bacterium, *P. gingivalis* impairs innate immunity in ways that alter the growth of the entire oral biofilm. These actions by the bacterium change the normally homeostatic host-biofilm cross talk, promoting a destructive, inflammatory shift in the host-biofilm interaction eventually leading to

periodontal diseases. *P. gingivalis* alone is not sufficient to cause periodontal disease, suggesting that the dysbiosis caused by *P. gingivalis* is the cause for the disease (Hajishengallis, Liang et al. 2011). Furthermore, this suggests that removal or targeting of the keystone pathogen is a possible way of treating periodontitis.

With the progression of periodontitis, *P. gingivalis* colonizes in the sub-gingival and gingival crevices and invades periodontal pockets. The toxins and proteases secreted by the bacterium further help to stimulate a pro-inflammatory response leading to the breakdown of oral epithelial tissue and bone. *P. gingivalis'* localization in the periodontal pockets further increases the release of inflammatory cytokines (such as IL-1 and TNF), matrix metalloproteinase, and reactive nitrogen and oxygen species by the immune system leading to further degradation of oral tissue (Graves, Cochran 2003).

Although the sub-gingival area and periodontal pockets are the favored niche of *P. gingivalis* it is exposed to hostile conditions in these areas. To be able to not only survive but grow in these conditions *P. gingivalis* has developed stress defense mechanisms for oxidative stress, nitrosative stress, and immune response evasion mechanisms. Furthermore, the environmental conditions in the mouth (pH, temperature, iron concentration, oxygen tension) are constantly changing. These stress responses are important for the virulence of *P. gingivalis*. Without the ability to adapt, the bacteria cannot survive in the oral cavity or inside host cells and cannot cause periodontal disease (Lewis et al. 2010, Lewis, Yanamandra et al. 2012, Boutrin, Wang et al. 2012).

Although *P. gingivalis* has primarily been implicated in periodontal disease, it has also been shown to cause disease states in other areas of the body. The bacterium has been implicated in rheumatoid arthritis; patients with rheumatoid arthritis have an

increased incidence of periodontal disease (Ogrendik, Kokino et al. 2005). High levels of *P. gingivalis* have been found in the amniotic fluid of women with premature labor and spontaneous abortion (Leon, Silva et al. 2007).

1.2.1 Virulence factors of *Porphyromonas gingivalis*

Porphyromonas gingivalis' role as a pathogenic bacterium has been studied extensively. To carry out this role, the bacterium has many tactics and virulence factors at its disposal. These factors help improve adherence mechanisms, regulate eukaryotic signals, and contribute to its virulence. Combined, they are essential to *P. gingivalis'* role in the development of periodontal disease.

Two types of fimbriae are found on *P. gingivalis*, major (long) and minor (short), both of which are important for attachment and adherence of the bacterium. Both major and minor fimbriae are immunogens involved in stimulating the inflammatory response of the host in periodontal disease. Major fimbriae are long, filamentous proteins on the cell surface that adhere to host tissues. They are capable of binding to various host cells such as epithelial cells and blood cells, causing the release of inflammatory cytokines (Amano, Nakagawa et al. 2004, Enersen, Nakano et al. 2013). Minor fimbriae are short proteins that are important in coadhesion and biofilm formation (Park, Simionato et al. 2005). Another important component of the outer membrane vesicle are lipopolysaccharides (LPS). Much like fimbriae, LPS can interact with host cell and host cell receptors and is an important inducer of the immune response (Grenier, Bertrand et al. 1995).

As previously stated, *P. gingivalis* is an asaccharolytic bacterium, meaning that it is incapable of using sugars or polysaccharides as an energy source and must use peptides. The bacterium secretes proteases as means to obtain the required nutrients for growth. These proteases are called gingipains and are secreted or membrane associated. There are two main types of gingipains: an Arg specific- which cleaves the carboxy peptide bond of an arginine residue, and a Lys-specific – which cleaves the carboxy peptide bond of a lysine residue (Okamoto, Misumi et al. 1995). The proteases are involved in nutrient acquisition, heme uptake, periodontal disease progression, and immune response evasion (Lewis 2010, Okamoto, Kadowaki et al. 1996, Belibasakis, Bostanci et al. 2007).

1.2.2 Interactions of *Porphyromonas gingivalis* with host cells.

Porphyromonas gingivalis is an invasive species of bacteria and has been shown to invade gingival epithelial cells *in vivo* (Lamont, Yilmaz 2002). Although the specific mechanisms are not known, the act of invading epithelial cells requires rearrangement of the cytoskeleton and the use of bacterial virulence factors. Fimbriae and adhesins expressed on the surface of *P. gingivalis* bind to surface receptors on epithelial cells where the rearrangement of microtubules and microfilaments is induced. The bacterial cell is engulfed into the epithelial cell where it can reproduce (Yilmaz, Watanabe et al. 2002). Furthermore, it is believed that bacterial secreted proteases play a role in invasion, although their exact function is not known.

Invasion plays an important role in the development of chronic periodontitis. Invasion into host cells is a tactic that has been adopted by other pathogenic bacteria. Its location inside the cell allows it to escape the effects of the immune system and

protects it from other stresses such as antibiotics. Hidden away inside the eukaryotic cell, *P. gingivalis* is afforded the opportunity to replicate and grow in a nutrient rich environment (Lamont, Chan et al. 1995). Although it is protected inside the host cell, it must still contend with the host cells defense mechanisms. One of these defenses, NO, is capable is diffusing through cell membranes and the invading bacteria must contend with the cells own NOS enzymes.

1.3 Hemoproteins

A hemoprotein is a metalloprotein containing the heme prosthetic group. The heme prosthetic group is an organic compound that allows the protein to carry out a role that it cannot do alone. Heme is a cyclic molecule that consists of an iron atom coordinated by 4 pyrrole groups, linked by methine bridges, forming a planar, highly hydrophobic porphyrin ring. The iron can have up to six coordination bonds: 4 bonds are to nitrogens of the 4 pyrrole groups, 1 to the side chain of the hemoprotein (generally a His or a Cys), and 1 typically to a ligand. The most common heme used in biology is iron coordinated by protoporphyrin IX (PPIX). Although iron is by far the most used metal in heme, it is possible for protoporpyrin IX bind other cations.

Hemoproteins have a diverse set of biological functions, including diatomic gas transport (hemoglobin), chemical catalysis (peroxidases), diatomic gas sensor proteins (FixL), and electron transfer (cytochromes) (Wandersman, Stojiljkovic 2000). Different hemoproteins respond very differently to the presence of the same ligand despite having a common prosthetic group. The variation is due to different axial ligation by protein side chains and a variety of secondary interactions, such as H-bonding, with residues in the heme pocket.

1.3.1 The role of Heme in *Porphyromonas gingivalis*.

Heme is required for growth of *Porphyromonas gingivalis* (Schifferle, Shostad et al. 1996). Heme and iron play necessary roles in the oxidative stress response (Henry, McKenzie et al. 2012), nitrosative stress response (Lewis, Yanamandra et al. 2012), and metabolism. Although it is a necessary component of many biological processes in the bacterium, it lacks the necessary mechanisms to synthesize the porphyrin ring. Furthermore, the concentration of iron, a necessary nutrient for almost all living organisms, *in vivo* is too low to support microbial growth. To rectify this problem *P. gingivalis* turns to scavenging iron and heme using various methods including proteolytic degradation.

1.3.2 Heme acquisition and uptake mechanisms

When heme is not readily available, the bacterium turns to other methods to obtain the valuable cofactor. The bacterium expresses gingipains which are a family of proteases/hemagglutinin complexes. The hemagglutinins have an active role in adhesion to and hemolysis of erythrocytes and constitutively have Arg or Lys protease activity. In addition to the protease-associated hemagglutinins, *P. gingivalis* can express a number of other proteins that are capable of adhering to erythrocytes. Once they are bound to the erythrocyte, hemolysins disrupt the cell causing the release of hemoglobin or other hemoproteins. The protease activity degrades the hemoglobin or other heme carrriers, leading to the release of free heme (Lewis 2010).

After it has been released, the heme must be transported into the cell. *P. gingivalis* encodes for 3 different heme uptake mechanisms: *ihtABCDE*, *Tlr,* and *hmu*.

(Fig. 4) *ihtABCDE* codes fo an iron-heme transport made up of 5 different protiens encoded by a single operon. *Tlr* is a Ton-B linked receptor that is similar to the *iht* encoded binding system, however it has a putative ATP-binding cassette for heme transport. The third transport, enconded by *hmu* operon, has recently been identified (Lewis 2010). Although they are vital to the survival and pathogenesis of *P. gingivalis*, the specific mechanisms used by the heme transport systems are not clear and being researched extensively.

1.4 NO and its role and biology

Nitric Oxide (NO) is a signaling and defense molecule in eukaryotic organisms. It is most notable for its role in the regulation of vasodilation in the cardiovascular system (1998 Nobel Prize in Physiology and Medicine) and its secretion by the immune system as a means to combat bacterial infection. NO is a free radical and can stabilize its unpaired electron two ways: reaction with species containing other unpaired electrons and interaction with the d-orbitals of transition metals, such as iron. In its reaction with iron, NO can form a rapid, stable, high affinity coordination bond with a ferrous iron in a heme group.

NO is uncharged and highly soluble in hydrophobic environments – a characteristic that allows it to freely diffuse through biological membranes. This not only makes it an excellent signaling molecule but a potent antimicrobial agent (Lancaster 1997).

1.4.1 Nitrosative stress and sources of nitrosative stress

Despite being a radical, NO is quite stable in biological environments depending on the components of the solvent and the concentration of oxygen (despite the common misconception that all free radicals are unstable and highly reactive) (Kroncke, Fehsel et al. 1997). Reactive nitrogen species act in conjunction with reactive oxygen species to damage cells. NO will react very quickly with other free radicals (Fig. 1). The reaction between superoxide and NO forms peroxynitrite, a very reactive, powerful oxidant that can damage proteins, lipids and DNA. It has been reported that the rate constant for the reaction of NO and O_2^- approaches the diffusion limit (Hill, Dranka et al. 2010,

Koppenol 2001). NO will react with most ROS, forming highly reactive products (Fig. 5). Ultimately, peroxynitrite is capable of degrading the very reactive and highly toxic hydroxyl radical (Fig. 1).

NO will also react with O_2 to form nitrite, nitrate, and nitrous anhydride. The intercom-version of these compounds can also be catalyzed by bacterial sources, of which NO is an obligate step. (Fig. 2). When we eat a meal, bacteria in our mouth and gut can produce nitrogen species as metabolic byproducts from nitrates present in our diet. Although not as reactive as peroxynitrite, high concentrations of nitrites and nitrates can be a source of nitrosative stress to hosts and bacteria. NO is capable of reacting with ammonia to stimulate the creation of hydroxylamine. Hydroxylamine is common mutagenic species that is capable of causing base-pair point mutation, and must be cleared.

NO is also synthesized by eukaryotic cells through the action of NO synthases or NOS enzyme. NOS enzymes catalyze the NADPH and O_2 dependent oxidation of arginine to citrulline and NO. The enzymatic synthesis of NO by the enzymes is complex and is dependent on many prosthetic groups and cofactors (Alderton, Cooper et al. 2001). Two types of NOS are relevant to bacterial infection:

(1) – eNOS (NOS3) – generates low levels of NO and is found in endothelial and epithelial cells among other cells types (such as cardiac myocytes and neurons)(Dudzinski, Michel 2007).

(2) – iNOS (NOS2) – inducible, generates the highest level of NO and is found in cells of the immune system that stimulate the inflammatory response (Kone, Kuncewicz et al. 2003).

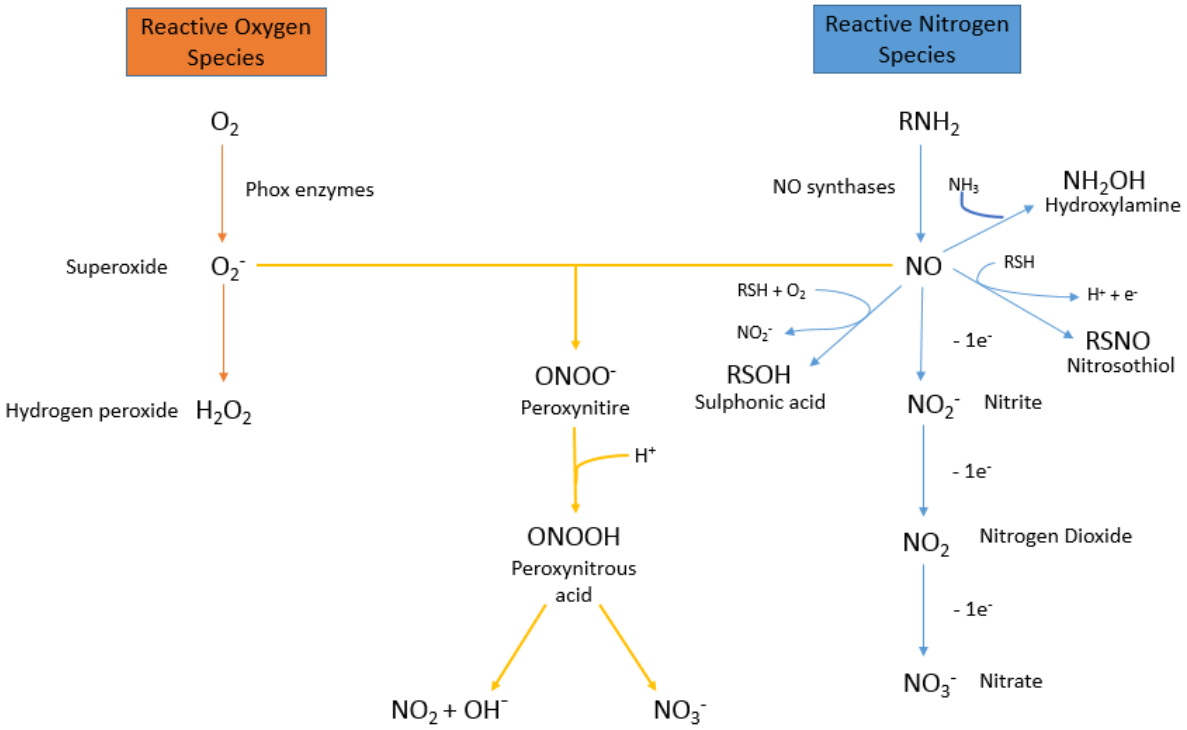

Figure 1 – Reactive Nitrogen and Reactive Oxygen species

Reactive nitrogen and oxygen species are dynamic, constantly changing and reacting based on the environment. This chart is mainly focused on reactive nitrogen species that can be harmful to bacteria.

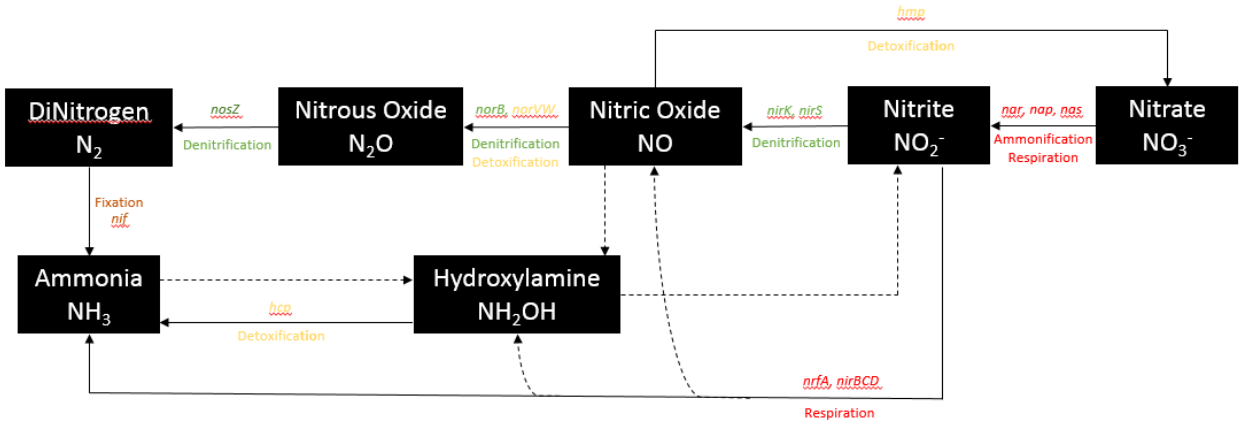

Figure 2 – The bacterial Inorganic Nitrogen Cycle Image adapted from Rodionov, D. A., Dubchak, I. L., Arkin, A. P., Alm, E. J., & Gelfand, M. S. (2005). Dissimilatory metabolism of nitrogen oxides in bacteria: Comparative reconstruction of transcriptional networks *PLoS Computational Biology, 1*(5).

1.4.2 Nitrosative Stress response

Bacterial cells must develop methods to protect cellular components from damage to reactive nitrogen species. Nitrosative stress responses detect increased concentrations of reactive nitrogen species and modulate the expression of necessary genes to clear the toxic species, usually through enzymatic means (Fang 2004). Several enzymes have been implicated in the detoxification of RNS in microbial species: microbial hemoglobins, nitrous oxide reductases, hydroxylamine reductases, and peroxynitrite reductases (Pathania, Navani et al. 2002, Gardner, Helmick et al. 2002, Bryk, Griffin et al. 2000, Boutrin, Wang et al. 2012). Furthermore, these antioxidant methods are required for infection in certain species.

1.5 Transcription factors and the regulation of stress responses in bacterial cells

Proper regulation of transcription is a necessity for all living cells. For a single cell organism it must be highly responsive due to how quickly the environment can change. Transcription factors are regulatory proteins that bind to a specific sequence of DNA, thereby controlling the expression of a gene at the transcriptional level. Transcription factors can promote, repress, or actively recruit RNA polymerase to an operon (Latchman 1997). A characteristic feature of transcription factors is the presence of a DNA binding domain that is specific for a sequence of DNA. This domain allows the protein to augment the flow of gene expression by binding directly to DNA (Ptashne, Gann 1997). The activities of many transcription factors are directly regulated by binding of a signal cytoplasmically or indirectly regulated by binding of extracellular proteins and peptides to cell-surface receptors. Structural analysis of many prokaryotic transcription factors has revealed that most are homo-dimers that bind to palindromic DNA sites (Huffman, Brennan 2002). Transcription factors regulate cell development, growth, differentiation, and coordinate stress responses. There are many transcription factors that are divided into families according to their DNA binding motif (helix-turn-helix, zinc finger), cofactor binding, and role (Pabo, Sauer 1992).

1.5.1 Transcription factors and stress response

Stress is a fact of life for bacterial cells. The environment which they inhabit can rapidly switch from good to bad: the pH may shift suddenly or nitrosative/oxidative stress may abruptly appear. Thus bacteria are constantly subjected to sources of potential stress. To cope, they must quickly express the necessary stress response genes and modulate expression of unnecessary genes. Many prokaryotic cells express

transcription factors that serve as sensor molecules. These proteins are activated indirectly (through the function of a membrane protein) or directly (direct binding of a metabolite or toxic molecule to the protein) and quickly change protein expression using their DNA binding domains. OxyR is a redox sensor in *E. coli* and many other microbes (Zheng, Storz 2000). The OxyR protein contains a thiol-disulfide redox switch to sense the presence of hydrogen peroxide allowing rapid activation of the protein. Once activated, the protein binds to specific palindromic sequences that are located upstream of the peroxidase and other antioxidant stress genes. Transcriptional activation then occurs through direct contact between OxyR and RNA polymerase (Zheng 1998). Although not all sensors/transcription factors follow this strategy, they all must employ a mechanism that allows for a rapid response to a change in the environment.

1.5.2 Hemoproteins as sensor proteins.

The ability of an organism to sense and respond to its environment is of utmost importance to its survival. Sensor proteins allow for physiological responses to environmental stimuli on a cellular level. Stimuli can include hypoxia, hyperoxia, or the presence of signaling molecules. A wide range of sensor proteins exists, many of which carry a cofactor. Over the years a wide and rapidly increasing range of heme-based sensor proteins have been discovered (Liebl, Lambry et al. 2013).

Heme proteins are nature's receptors for the gaseous CO, NO, and O_2 molecules. These gaseous XO molecules play important roles in many biological processes such as signaling and metabolism. The heme prosthetic group acts as a binding platform for the diatomic gases, performing a role that protein could not do on its own. By binding to the heme, the XO molecules can trigger a protein conformational

change that can initiate DNA binding or an enzymatic reaction and allow the organism to react in an appropriate manner. The surrounding protein and its side chains in the heme pocket are critical in determining the specificity among the gaseous XO molecules and for guiding the subsequent protein conformational change. Steric contacts can directly influence ligand binding and distort the porphyrin ring, influencing the Fe-XO binding properties (Spiro, Soldatova 2012, Spiro, Soldatova et al. 2013).

In principle, heme based gas sensors act as bi-stable switch proteins. The switching from one state to the other is initiated by binding of the gaseous XO ligand to, or dissociation from, the heme (Fig. 3). The switching from an inactive to an active state are well-defined biochemical events that intrinsically take place on the timescale of bond vibrations (Liebl, Lambry et al. 2013).

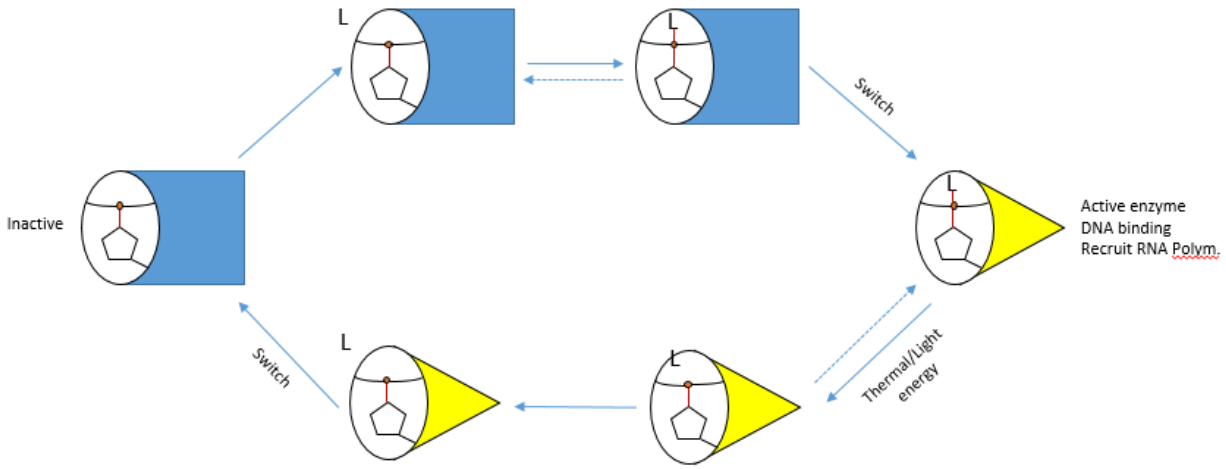

Figure 3 - General scheme of inter-protein signal transition of a heme sensor

Image adapted from Liebl, U. et al, 2013. Primary processes in heme-based sensor proteins. Biochimica et Biophysica Acta (BBA) - Proteins and Proteomics. 1834: 1684-1692. Heme sensor proteins are bistable switch proteins. Binding of ligand, such as NO, induces a conformational change in the protein, promoting the active state. The conformational change occurs on the order of bond vibrations. The protein performs a role while active. Loss of the ligand binding causes the protein to revert to the inactive state.

1.6 Nitrosative Stress and *Porphyromonas gingivalis*

There are multiple sources of nitrosave stress in the oral cavity. Nitrite concentrations can range from 10 μM to more than 1 mM (Lundberg, Weitzberg et al. 2004). Nitrite is produced by oral bacteria as a byproduct of metabolism and dietary intake of nitrate and nitrite rich foods is the main source of reactive nitrogen species in the oral cavity. Nitric oxide may be generated by nitrite in the oral cavity through the bacterial respiratory nitrite reductase system NrfHA (Spiro 2006, Hammes 2012) (Fig. 2). Intake of food that lowers the pH of the oral cavity creates favorable conditions for the conversion of nitrite to nitric oxide (Palmerini, Palombari et al. 2003). The innate immune system incorporates mass NO production as part of its response to bacterial infection. Bacterial invasion of endothelial cells causes an increase in NO production by their type 3 NOS enzymes. To survive in the periodontal pocket, *P. gingivalis* must have mechanisms to circumvent nitrosative stress from multiple sources.

The nitrosative stress response in *P. gingivalis* remains poorly understood. Recently, it has been shown that an Hcp (hybrid complex protein) plays a significant role nitrosative stress resistance (Boutrin, Wang et al. 2012). Hcp is a putative hydroxylamine reductase that is expressed during conditions of nitrite and nitrate stress and has been shown to be up-regulated in high concentrations of NO. Hcp has been extensively studied in other anaerobic and facultative anaerobic bacteria (van den Berg, Hagen et al. 2000, Beliaev, Thompson et al. 2002). Hydroxylamine is a toxic byproduct that can be created during nitrite ammonification. Nitric oxide catalyzes the reduction of ammonia yielding hydroxylamine. Hcp detoxifies hydroxylamine by converting it to water and ammonia.

1.6.1 HcpR's role in the nitrosative stress response in *Porphyromonas gingivalis*

The response to nitrosative stress is regulated by FNR (fumarate-nitrate regulator) and FNR-like proteins in many bacteria, including *E. coli*. These regulators are structurally related to cyclic AMP receptor protein (CRP) and fumarate and nitrate reduction regulator (FNR) from *E. coli* (Schultz, Shields et al. 1991, Spiro 1994). All members of this family are homo-dimers that are composed of 3 domains: a sensing domain that typically utilizes an iron-sulfur cluster, a dimerization helix, and a DNA binding domain. The members of this family control many important pathways in a wide variety of bacterial species; these include (but not limited to) hypoxia, oxygen exposure, oxidative stress and nitrosative stress. HcpR is a novel FNR-like regulator that is predicted to regulate the expression of *hcp* and other genes responsible for denitrification. It lacks the conserved cysteine residues required for binding of the Fe-S cluster seen in FNR and its homologues. HcpR has been shown to control the expression of Hcp in the *Desulfovibrio* species of anaerobic bacteria and is proposed to be present in many other bacterial species such as *Baccteroidetes*, *Geobacter,* and *Thermotogales* (Rodionov, Dubchak et al. 2004, Arai, Mizutani et al. 2003, Cadby, Busby et al. 2011).

HcpR is believed to help coordinate the nitrosative stress response in *P. gingivalis*. Under conditions of NO or nitrite stress *hcp*, a putative hydroxylamine reductase, (PG0893) has been shown to be up-regulated (Boutrin, Wang et al. 2012). HcpR has been shown to bind directly to the *hcp* promoter. Knockout of the putative HcpR gene (PG1053) in *P. gingivalis* W83 nullifies the up-regulation of Hcp under conditions of nitrosative stress. Furthermore, growth of the knockout strain was greatly

reduced in the presence of nitrite and NO and did not survive with host cells, revealing that HcpR plays a vital role in the virulence of *P. gingivalis*. The nitrosative stress response was also shown to be dependent on heme, implying that heme may play a role in detoxification or recognition of the diatomic gas molecule NO. Up-regulation of the major heme uptake gene *hmuY* (PG1553) was seen in the presence of NO generating agents. Furthermore, hemin is required for binding of recombinant-HcpR to the *hcp* promoter (Lewis, Yanamandra et al. 2012). Bioinformatics studies of the gene product of *P. gingivalis*-HcpR reveal that it is related to DNR, an FNR like transcription factor that plays a role in the nitrosative stress response in *Pseudomonas aeruginosa* (Giardina, Rinaldo et al. 2009, Castiglione, Rinaldo et al. 2009).

DNR is a member of the FNR superfamily of transcription factors. It is a sensor protein that lacks the conserved cysteine residues necessary to form the Fe-S cluster; instead it utilizes the heme cofactor to bind the diatomic gas molecule NO. It is theorized that direct binding of NO stimulates the activation of the protein allowing it to modulate expression of genes responsible for denitrification, although the exact mechanism of activation is not understood (Castiglione, Rinaldo et al. 2009). HcpR appears to play a similar role in *P. gingivalis*. The exact mechanisms that govern the nitrosative stress response in *P. gingivalis* are not understood even though they are important aspect of the micro-organism's survival and virulence.

Chapter 2 – Hypothesis and Aims

2.1 Hypothesis

HcpR is a sensor transcription factor that is a vital part of the nitrosative stress response in *P. gingivalis.* HcpR is a homodimer, heme binding protein that utilizes the heme-bound iron to bind the diatomic gas molecule NO, a reactive nitrogen species and one of the causative agents of nitrosative stress in mouth and periodontal pocket. Binding of NO to HcpR bound heme causes a change in the oxidation of Iron(III) to Iron(II) producing a conformational change of the protein that allows the protein to modulate expression of genes at a promoter upstream of a target gene.

2.2 Aims

The main goal of this project is to characterize HcpR and better understand the mechanisms it uses to regulate the nitrosative stress response in *Porphyromonas gingivalis.* The following specific aims have been performed to attain this goal:

Aim 1: Use bioinformatics resources to construct a molecular homology model and analyze the primary sequence of HcpR. Bioinformatics is a good starting point, and we will use a number of bioinformatics resources at our disposal to understand the structure and function of the protein.

Aim 2: Determine the oligomeric state of HcpR. Most prokaryotic transcription factors are dimers in solution. Understanding the stoichiometry of the protein is necessary for a basic understanding of its behavior.

Aim 3: Analyze the heme binding properties of HcpR. Predictions suggest that HcpR belongs to a class of regulators that utilize heme as a sensor for nitrosative stress. UV-Vis spectroscopy, CD spectroscopy, TMBZ assays, and Fluorescence assays will be used to analyze the heme binding properties.

Aim 4: Analyze the NO binding properties of HcpR. To be an efficient regulator, the protein must bind a ligand to stimulate a response. Anaerobic UV-Vis spectroscopy and Resonance Raman spectroscopy will be used to analyze the NO binding properties.

Aim 5: Analyze the structure of HcpR. To fully understand the mechanisms of HcpR, information on the structure must be obtained. SAXS will be employed to gain some knowledge on the structure of HcpR. We will also attempt to crystallize HcpR and solve its structure.

Aim 6: To further ascertain the biological significance of HcpR, the creation of a promoter assay will allow for the quantification of efficiency of the activation of HcpR.

Chapter 3 – Materials and Methods

3.1 – Bioinformatics

Using the protein Basic Local Alignment Search Tool (PBLAST) on the HcpR sequence, an FNR-like regulator in *Pseudomonas aeruginosa* with a similar sequence was found (Lewis, Yanamandra et al. 2012); a partial crystal structure of DNR has been solved (PDB 3DKW). Using DNR as a template and the one-to-one threading method of Phyre protein folding server (Kelley, Sternberg 2009), a 3-Dimensional homology model of HcpR was constructed. Chain A of DNR was used as a template, and dimer homology model was made by using the match-maker function in UCSF chimera using DNR chains A and B as a template (Pettersen, Goddard et al. 2004). InterproScan5 was used to match the sequence of HcpR against a number of databases to predict conserved domains of the protein (Jones, Binns et al. 2014).

3.2 – Cloning and Expression

The sequence of the *HcpR* gene (PG1053) was identified in the Oralgen W83 *Porphyromonas gingivalis* genome database (oralgen.org). Primers were designed and the *hcpR* gene was PCR amplified from W83 *P. gingivalis* genomic DNA. Three vectors were chosen for expression: the pFC20K HaloTag T7 SP6 flexi vector (Promega Corporation), pET30-A and a modified pET21-A vector (provided by Dr. Peterson). The primers for cloning into the pFC20K vector were engineered to have *SgfI* (forward) and *EcoICRI* (reverse) restrictions sites (Table I). The primers for cloning into the m-pET21 vector were engineered to have *BamHI* (forward) and *XhoI* (reverse) restriction sites and amplified the full length gene (Table I).

The DNA amplified with the m-pET primers was cloned into the m-pET21d vector to create m-pET21-*hcpR.* The PCR product and vector were digested with *BamHI* and *XhoI* and gel purified. The digested fragments were ligated with T4 DNA ligase (Life Technologies) and transformed into TOP10 cells (Life Technologeis) for antibiotic resistance screening. A successful clone was identified and sequenced. The clone was engineered to have a tail of six histidines attached to the carboxy terminus of the gene product. The m-pET21d sequence contains a TEV protease cleavage site between the end of the *hcpR* gene sequence and the His tag. This cleavage site was used to remove the His tag after purification.

The DNA amplified with the HcpR-halo primers was cloned into the pFC20K vector to create Halo-*hcpR*. The PCR product was digested with SgfI and EcoICRI; the vector was digested with SgfI and PmeI. The fragments were gel purified and ligated using T4 DNA ligase. The ligation product was transformed into DH5-alpha competent *E. coli* (Bioline) for antibiotic resistance screening. A successful clone was identified and sequenced. The clone was engineered to place the Halo tag sequence at the carboxy terminus of the gene product. The Halo tag is an 890 b.p. region that codes for an antibody binding domain which is used for immunoprecipitation; between the Halo tag and 3' end of the wt-*hcpR* there is a TEV cleavage site used to remove the tag from the protein.

Cloning and production of the pET30-*hcpr* plasmid are detailed in Lewis, Yanamandra et al. 2012.

Table I – Primers used in this Study

m-pET-*hcpR*-Forward	CTTCCAGGGATCCCCAGAATTCGATCTTC
m-pET-*hcpR*-Reverse	GCGCACTCGAGTTACTCCAGCCTCGACA
Halo-*hcpR*-Forward	TTGTGTTTAAACCTCCAGCCTCGACAA
Halo-*hcpR*-Reverse	GCCGGCGATCGCCATGGATCCCGAAT
pACYc-184-*hcpr*-Forward	CCGTCACCCAGGATGCTGTAGATGGATCCCGAATTCGATCTTC
pACYc-184-*hcpr*-Reverse	CCATCCAGCCTCGGGTCGCGATTACTCCAGCCTCGACAATC
pACYc-Sequencing-F	TGAAGTCAGCCCCATACGAT
pACYc-Sequencing-R	GGCATAAATCGCCGTGAC

Table 2 – Vectors used in this study

pET30-*hcpR*	pET30 vector with *hcpR* insert. Contains a Strep tag and His-Tag on the N-terminal region.
m-pET21-*hcpR*	Modified pET21 vector with HcpR insert. The vector removes N-terminal S-Tag and adds a TEV site to cut off C-termianl 6x His tag .
Halo-*hcpR*	pFC20K with the HcpR insert. Adds a halo antibody tag on the C terminal region for immunoprecipitatio. TEV site used to remove tag.
PACYc-184-*hcpR*	PACYc-184 vector with *hcpR* insert used for promoter studies.. A low copy vector at roughly ~15 copies per cell.
PUC57	A high copy vector that contains the promoter constructs used for the promoter studies.

The m-pET21-*hcpR* and pET30-*hcpR* plasmids were transformed into BL21 (DE3) *E. coli* (Bioline) for expression. The Halo-*hcpR* plasmid was placed into KRX *E. coli* (Promega) for expression.

The m-pET21-*hcpR* and pET30-*hcpR* in BL21 (DE3) were grown in Luria-Bertani (LB) broth or self-induction media (recipe in appendix) with shaking (225 RPM) at 37 °C. At mid log phase (~0.6 OD at 660 nm) the LB cultures were induced with a final concentration of 1 mM IPTG and grown overnight. The self-induction media cultures were grown overnight with shaking (225 RPM) at 37°C. The Halo-*hcpR* in KRX *E. coli* was grown in LB broth with shaking (225 RPM) at 37 °C. At mid log phase the culture was induced with a final concentration of 0.008% of L-rhamnose and grown overnight.

3.3 Purification of HcpR

3.3.1 His-tag Purification

After growth and induction the cells were spun down at 12,000 RCF and washed with PBS. Cell pellets were suspended in binding buffer (50 mM NaH_2PO_4, 300 mM NaCl, 10 mM imidazole, pH 8.0) and 100 mg of Lysozyme was added. The lysis solution was incubated on ice for 30 minutes. After incubation the cells were sonicated. The cell lysates were centrifuged at 15000 RPM to pellet cell/cell debris. The lysates were passed through a column containing a Ni-NTA Resin (Qiagen) equilibrated with binding buffer. The column was washed with 200 mL of wash buffer (50 mM NaH_2PO_4, 300 mM NaCl, 25 mM imidazole, pH 8.0). The protein was eluted from the column with 250 mM imidazole solution. The elutions were run on a 10% SDS-PAGE gel to check for purity.

Elutions were dialyzed to remove excess imidazole and tag was cut off the purified HcpR using TEV protease (kindly supplied by Dr. Peterson) at room

temperature. The completeness of the TEV cleavage was monitored using SDS-PAGE gels. Once cleavage was complete, the purified protein was applied to the Ni-NTA column and incubated with the resin for 15 minutes, before eluting the untagged, purified HcpR. The purified protein was stored at -80 ºC.

3.3.2 Halo-tag Purification

Induced cell cultures were spun down and suspended in purification buffer (50 mM Hepes, 150 mM NaCl, 1 mM DTT, pH 7.0). Cells were lysed using cell-lytic B reagent lysis reagent (Sigma-Aldrich). To each sample, 10 units of benzonase (Sigma-Aldrich) were added to degrade genomic DNA. The cell debris was spun down and the cell lysate was added to Halo-link resin (Promega). The cell lysates were incubated with the resin for 1 hour at room temperature with inversion. After incubation, the sample was washed with 50 mL purification buffer via batch method: samples were spun down and supernatant removed and 10 mL of buffer added. HcpR was eluted from the resin by adding TEV protease to the resin and inverting at 4°C overnight. Elutions were analyzed on SDS-PAGE gels. The purified protein was then stored at -80°C.

3.3.3 Reconstitution of purified HcpR with Heme

Purified HcpR was reconstituted with 1.5 molar excess of heme in 0.1 M NaOH. The mixture was incubated for 30 minutes - 1 hour at room temperature. Dialysis was used to remove excess heme and salt.

3.4 Native Gel electrophoresis

Native gel electrophoresis was done using the recombinant protein purified from *E. coli* cntaining pET30-*hcpR*. The sample protein was not de-tagged. A Tris-Acetate

polyacrylamide gel was run in 50 mM Tris-Glycine buffer for approximately 2 hours. Apo, Heme, and DNA-complex HcpR were run at varying amounts.

3.5 Analytical Ultracentrifugation

HcpR was purified using the Halo method as described before and dialyzed into 50 mM Hepes, 150 mM NaCl, and 1 mM DTT. Apo HcpR was diluted into 4 different concentrations: 0.1 mg/ml (2.0 μM), 0.2 mg/ml (3.9 μM), 0.5 mg/ml (9.8 μM) and 1.0 mg/ml (19.6 μM). A Beckman Optima XL-I analytical ultracentrifuge was used to analyze the samples. The velocity sedimentation experiment was run at 4000, 5000, and 7000 RPM in a four-position AN-60Ti rotor at 20°C in aluminum double sector cells. Concentration profiles were recorded using UV absorption (280 nm and 260 nm).

3.6 TMBZ assay

To test for the presence of heme binding to HcpR, 15 μg of reconstituted HcpR was run on a native 10% polyacrylamide gel. Hemoglobin was used as a positive control and *P. gingivalis* OxyR was used as a negative control. The gel was run for approximately 1 hour in 50 mM Tris-Glycine running buffer. After running, the gel was soaked in TMBZ (tetramethylbenzidine) for 30 minutes. The TMBZ was poured off and the gel cleaned with water. Hydrogen peroxide (3%) was then applied to the gel. The presence of heme was marked by a blue-green stain.

3.7 UV-Vis studies

Heme was titrated with varying dilutions of purified apo HcpR (Fig. 16) to observe spontaneous binding to HcpR. Sample buffer was 25 mM Phosphate, 100 mM NaCl at pH 7.0. The samples were scanned from 200-800 nm using a Thermo Biomate 3S UV-Vis spectrophotometer. To study anaerobic effects of heme binding Apo-HcpR was

made anaerobic by placing in an anaerobic atmosphere chamber. Anaerobic heme solution was added to the sample in a 1:1 ratio and the sample was scanned from 200-800 nm in a sealed quartz cuvette.

Reconstituted HcpR was dialyzed into 25 mM Phosphate, 100 mM NaCl, and 1 mM TCEP. The samples were placed in an anaerobic chamber and 10 mM Dithionite was added to the samples. The samples were incubated overnight in the chamber then passed through a PD-10 desalting column (GE healthcare) to remove excess dithionite. NONOate was used to prepare nitrosylated samples. 20 mg of NONOate was dissolved in 100 µL buffer and NO formation was observed by the formation of bubbles in solution. Nitrosylated samples were prepared by adding 50 µL of dissolved NONOate to 450 µL of 1 mg/mL HcpR sample. Samples were placed in sealed quartz cuvettes to maintain integrity of the anaerobic samples and scanned from 280-800 nm.

3.8 Fluorescence Studies

To test for heme binding a time scan titration was performed using heme to titrate HcpR. A 1 mg/ml sample of Apo-HcpR was titrated with 20 µL of 1 mg/ml solution of heme. The sample was excited at 280 and the emission was monitored from 300 to 460.

To better understand the binding properties, a standard curve was constructed to define the binding parameters. Purified HcpR was dialyzed into 25 mM Hepes, 100 mM NaCl, and 2 mM TCEP. A heme dilution series was constructed keeping HcpR constant at 6.667 µM. The samples were excited at 280 nm and emission was observed at 340 nm. A quartz cuvette was used for analysis in an ISS PC1 fluorimeter.

3.9 CD Studies

Apo and Heme forms of HcpR at 0.5 mg/mL (9.8 μM) were used for CD studies over a spectrum of 170-260 nm wavelength. Buffer was 25mM Phosphate, 50 mM NaCl, pH 7.0. An Olis DSM 1000 CD spectrophotometer was used to collect the data in quartz cuvettes. All samples were collected at room temperature.

Analysis of NO binding was done under anaerobic conditions. 5mM of dithionite was added to the heme-HcpR. The samples were nitrosylated by using 10 mg NONOate added directly to the sample. The cuvette was capped in an anaerobic chamber. Spectrum of both anaerobic nitrosylated and anaerobic non-nitrosylated samples were generated in 170-260 nm range. All samples were collected at room temperature.

3.10 Resonance Raman Studies

HcpR was purified using the 6x His tag method as previously described and heme-reconstituted as previously described. The samples were dialyzed into purification buffer (25 mM Tris, 100 mM NaCl, and 2 mM TCEP at pH of 7.5) and concentrated down to 20 mg/ml (392 μM). 5 mM dithionite was added to the samples and then placed under anaerobic conditions overnight. After overnight anaerobic exchange, NONOate was used to nitrosylate samples. The samples were put in glass melting point capillaries under anaerobic conditions and sealed. The spectra were obtained with a krypton ion laser at 406.7 nm (Coherent Sabre DBW laser). The detection system used was a liquid N_2 cooled 400 x 1340 CCD detector (Princeton Instruments, Roper Scientific, Trenton, NJ) and a 0.5 m spectrograph (Spex model 1870; Horiba/Jobin-Yvon, Edison, NJ) set to 100 um slit width and fitted with an 1800 or 2400 L/mm holographic grating (Jobin-Yvon). GRAMS/AI version 7.0 was used to perform spectral baseline leveling by a fifth

order polynomial routine. The mathematical peak fitting module of Origin Pro version 7.5 was used to deconvolute band shapes and generate the spectral graph.

3.11 Small Angle X-ray Scattering

Recombinant HcpR was purified and sent to the SIBYLS beamline at the Lawrence Berkeley National Laboratory. A concentration gradient of 0.5 mg/ml, 1.0 mg/ml, and 2 mg/ml of Apo and DNA-complex HcpR and 0.25 mg/ml, 0.5 mg/ml, and 1 mg/ml of the Heme-HcpR was exchanged in 25 mM Tris, 100 mM NaCl, and 2 mM TCEP at pH 7.5 buffer. Each form of the protein was dialyzed against 2 L of the buffer overnight before being sent off. The matching buffer was sent with it. The ATSAS package was used to analyze the scattering profiles and create the Kratky, Guinier, and distance-distribution function graphs. DAMMIF was used to create the ab initio models. The FoXS server was used to create a theoretical scattering curve of the HcpR homology model.

3.12 Promoter Studies

The *hcpR* gene was cloned into the pACYC184 vector (New England Biolabs) under the constitutive *tet* promoter yielding the plasmid pACY-*hcpR*. The *hcpR* PCR product was engineered to add *SfcI* (5'-end) and *NruI* (3'-end) restriction sites (enzymes from NEB). Vector and PCR product were digested, gel purified, and ligated. Ligation product was transformed into TOP-10 *E. coli* (Life Technologies) for antibiotic resistance screening on chloramphenicol plates. A successful clone was identified and sequenced. Three reporter systems were created using the P-glow Bs2 gene. The Bs2 gene carries the DNA sequence of a truncated YtvA from the blue-light photoreceptor of *Bacillus subtilis* which is optimal for using in anaerobic conditions. It encodes only the photoactive LOV domain optimized for usage in *E. coli.* The molecular weight is 19 kDa and the protein forms homodimers in

solution. The Bs2 gene was placed downstream of the hcp promoter of *Porphorymonas gingivalis* creating the construct pUC-GLOW-PG. Two other constructs were created: the DNR binding site of the *Pseudomonas aeruginosa nor* promoter was replaced with the HcpR binding site and placed upstream of the Bs2 gene creating pUC-GLOW-PA; the FNR binding site of the *E. coli melR* promoter was replaced with the HcpR binding site and placed upstream of the Bs2 gene creating pUC-GLOW-EC. All 3 constructs were synthesized (Genescript) and placed into the pUC57 vector. The promoter-reporter recombinant genes were flanked with NdeI (5' end) and BamHI (3' end) restriction sites.

Each reporter construct was co-transformed into TOP-10 *E. coli* with the pACY-*hcpr* construct. Overnight cultures of each strain were used to inoculate 20 mL LB broth. Each culture was grown at 37°C with shaking (225 RPM) to OD_{660} 0.5 and were placed in an anaerobic chamber. The cultures sat in anaerobic conditions for 30 minutes to remove oxygen. The cultures were distributed into a 96 well plate, and pipetted vigorously to remove residual oxygen. A gradient of an increasing amount of NONOate dissolved solution or nitrite was added to each well. After a 1 hour incubation, the cells were measured for the fluorescence via excitation at 450 nm and emission at 495 nm.

3.13 Crystal Screening

A wide range of conditions were screened by hand to obtain a crystal of the native-HcpR using hanging drop vapor diffusion, sitting drop diffusion, and oil diffusion methods. A number of commercially available crystallization screens were employed: Crystal Screens 1 and 2 (Hampton Research), Natrix Screen (Hampton Research), Wizard Classic Crystallization screens 1, 2, and 3 (Rigaku reagents). Screens were placed at 20ºC, 16ºC, and 4ºC.

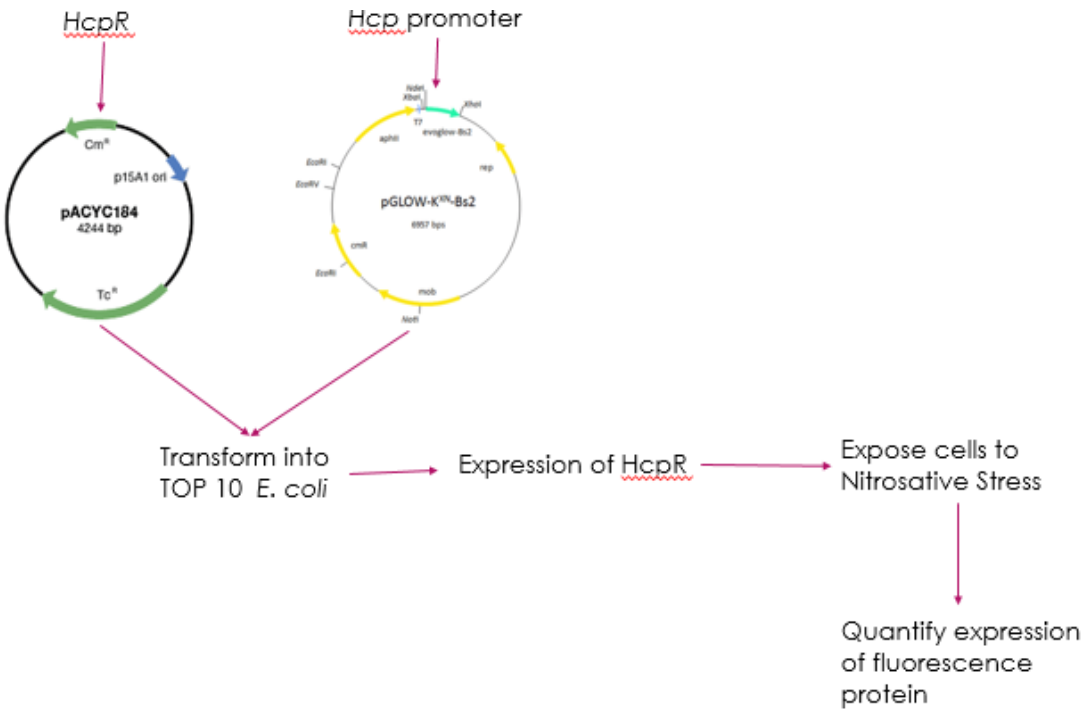

Figure 4 – Schematic overview of promoter study

hcpR will be cloned into the pACY184 plasmid, a vector that has a low copy number (and thus a low expression). The pACYC-*hcpR* vector will be co-transformed into *E. coli* with a vector containing a fluorescent reporter gene downstream of the hcp promoter (vectors detailed in figure 5). The bacteria will be stimulated with reactive nitrogen species and the expression of the reporter gene will be quantified.

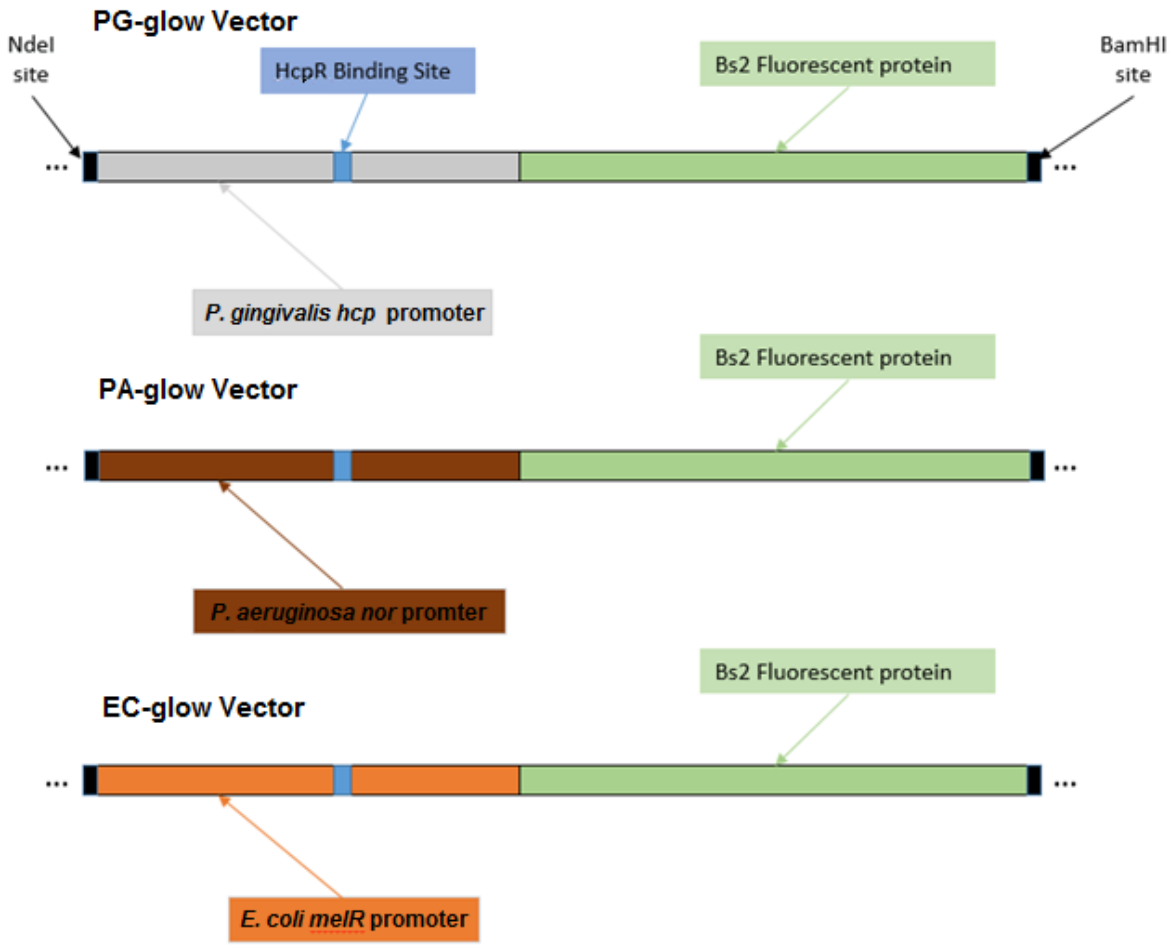

Figure 5 – Construct used in promoter studies

There are 3 reporter constructs utilized in this study; each construct utilizes the BS2 fluorescent reporter gene downstream of a promoter. Three promoters are used: the *P. gingivalis hcp* promoter; the *P. aeruginosa nor* promoter; the *E. coli melR* promoter. The DNR binding site was replaced in the *nor* promoter with an HcpR binding site and the FNR binding site in the *melR* promoter was replaced with an HcpR binding site.

Chapter 4 – Results

4.1 Bioinformatics results

The Apo-HcpR homology model was based on the Apo-DNR crystal structure. DNR is a heme-binding sensor protein that regulates the nitrosative stress response in *Pseudomonas aeruginosa*. DNR oligomerizes as a dimer in solution, however the unit cell of the crystal structure is an octamer of 4 dimers (PDB 3DKW). Chain A of DNR and the HcpR homology model were over-layed using the match-maker function of Chimera: the RMSD between the homology model and DNR-chain A is 0.179 (Fig. 6-7). The low RMSD indicate a high structural similarity. Using the QMEAN server for homology model estimation, it should be noted that the energy levels for HcpR aren't as low as DNR. This indicates that although it is a good match, there is some forced positioning. Most of the variation between the homology model and DNR is in the N-terminal DNA binding region.

The HcpR homology model is made up of 3 domains: an N-terminal Ligand Binding Domain, a dimerization helix, and a C-terminal DNA binding domain (Fig. 8). Residues 1-125 form the heme binding domain. The ligand binding domain forms a pocket structure that has a high number of hydrophobic residues, which are most likely needed for binding of the highly hydrophobic heme cofactor (Fig 9). Residues 126-171 forms the dimerization helix. The residues along the central helix form a high number of interactions, creating a tight bonding between the two subunits. Residues 172-228 forms the DNA binding domain which contains a helix-turn-helix DNA binding motif. This specific motif is a common trait among members of the FNR-like superfamily.

The InterProScan returned results that reaffirm the conclusions from the homology model (Fig. 10). The N-terminal region of HcpR resembles that of a Cyclic-nucleotide binding domain; this is a common theme among members of the CRP-FNR superfamily. The C-terminal region of HcpR resembles a CRP helix-turn-helix DNA binding domain.

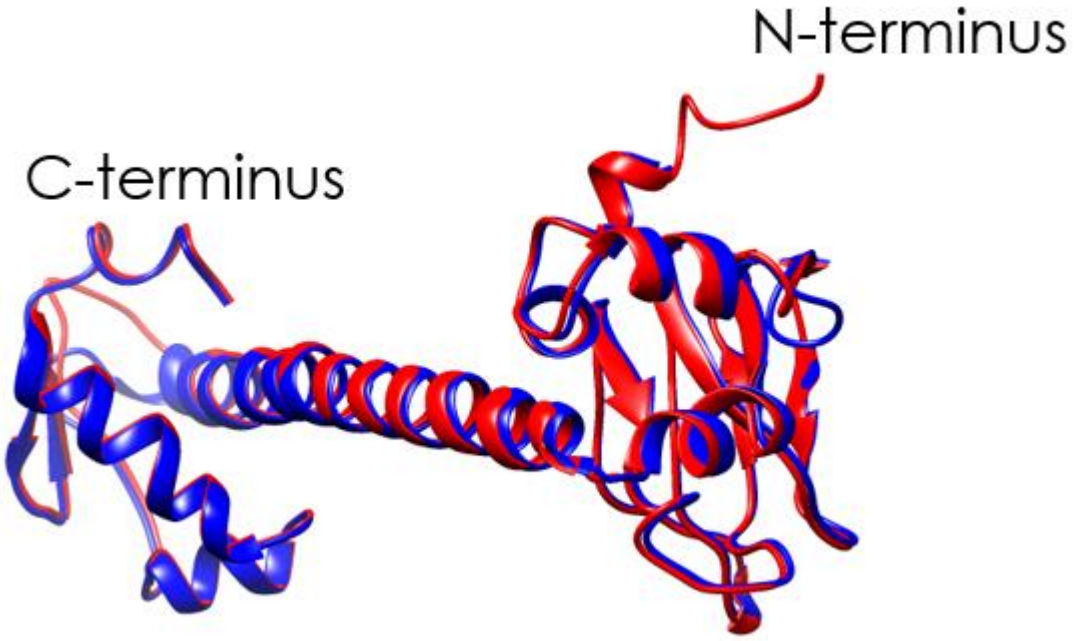

Figure 6 – Superimposed structures of HcpR and DNR

All images generated using UCSF Chimera. The HcpR homology model (Blue) is overlayed with DNR crystal structure (Red) (PDB: 3DKW) with an RMSD value of 0.179.

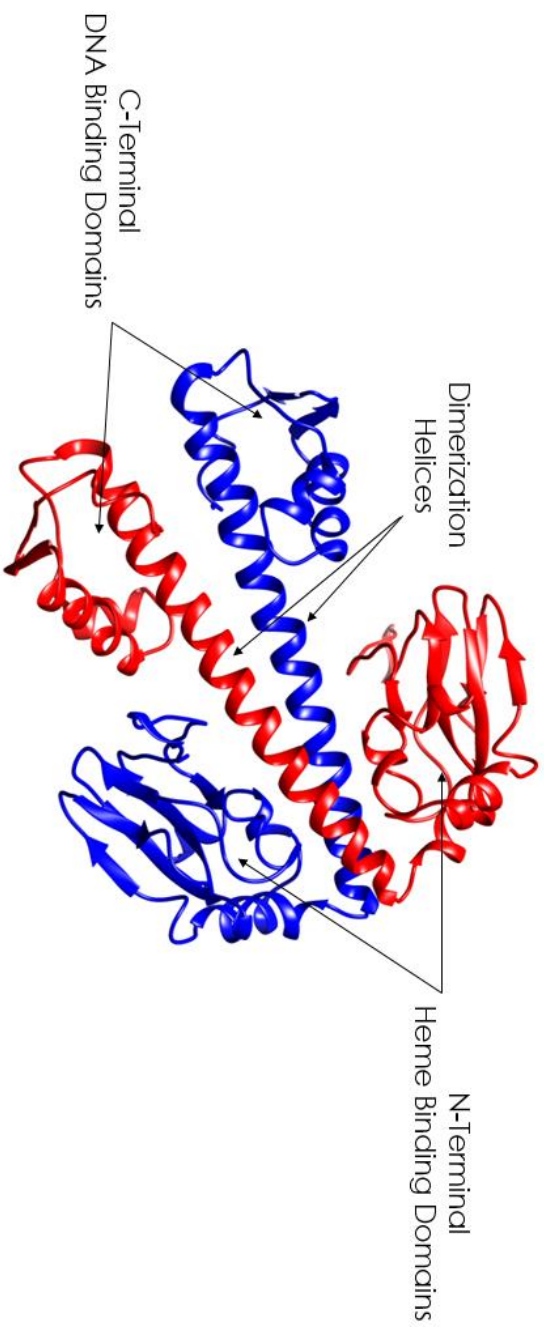

Figure 7 – Dimeric homology model of HcpR

The model is a homo-dimer made up of two identical strands. The predicted homo-dimer of HcpR was modeled after the crystal structure of the DNR homodimer.

A

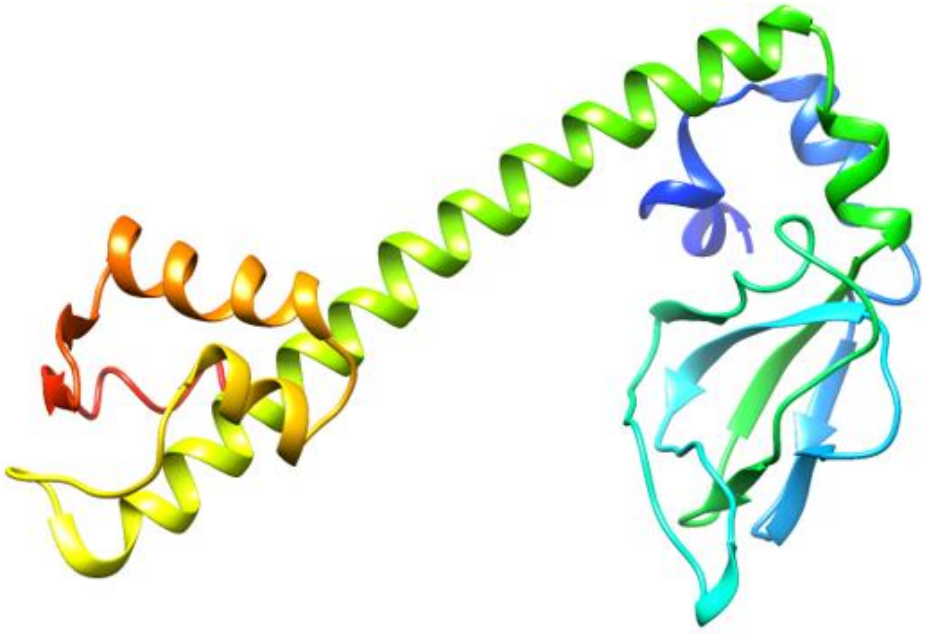

B

MDPEFDLLK AWKSSGLSVG MKDDELLALL ESCSYRVERL
KAEELYAIGG DKLQDLRIVGV GEIRAEMVG PSGKQILIDT
LAVGRILAPA LLFASENILP VLFANEDSV LFRIGKEEFK
GMMHKYPTLM ENFIGMISDI SAFLMKKIHQ LSLRSLQGKI
GDYLFQLYTK DGSNRIVVE SSWKELSDRFG VNRQSLARSL
SQLEEEGIIR VDGKSIEILQ PNRLSRLE

Figure 8 – Domains of HcpR homology model

The HcpR homology model (A) is made up of an N-terminal heme binding domain, a C-terminal DNA binding domain, and a dimerization helix that links the two domains. The sequence of HcpR (B) is below and highlighted based on its domain. Text - Blue: N-Terminal ligand binding domain; Green: dimerization helix; Red: C-temrinal DNA binding domain.

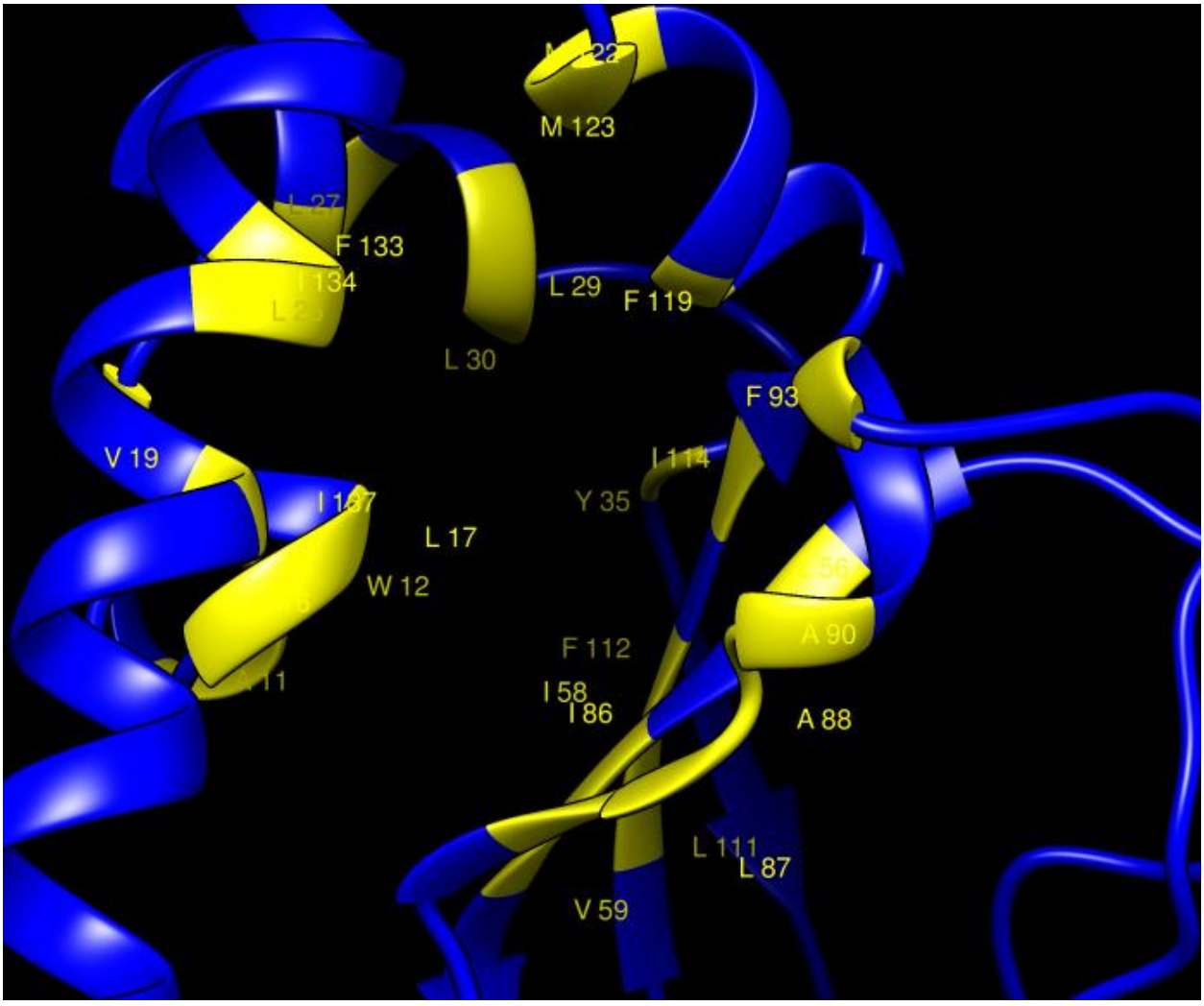

Figure 9 – Hydrophobic residues in the Heme binding pocket

Hydrophobic residues in the postulated heme binding domain are highlighted in yellow. The protoporphoryin IX ring of heme is very hydrophobic, other heme binding proteins typically hold the cofactor through mainly hydrophobic interactions.

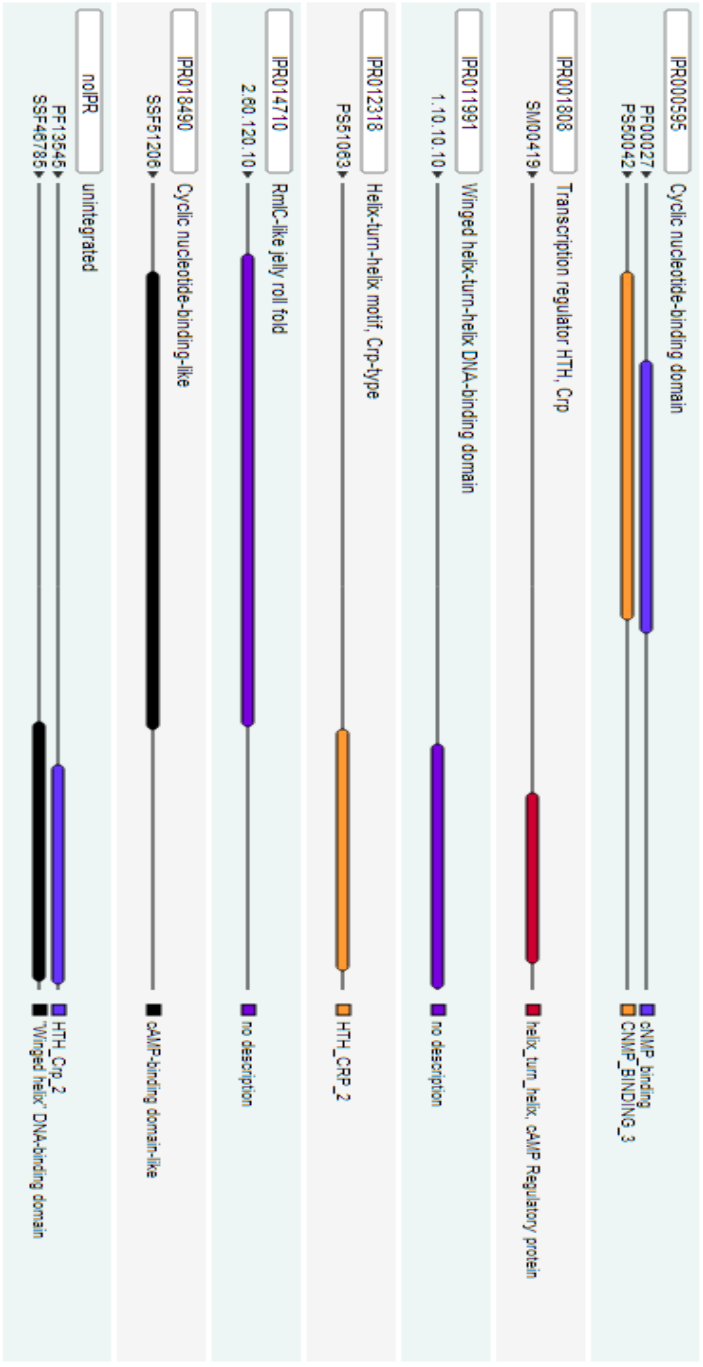

Figure 10 – InterProScan 4.8 Results

InterProScan returns results from a number of databases that are used to scan the query sequence. The database used for each line is color coded with the legend at the bottom of the figure.

4.2 Expression and Purification of recombinant HcpR

A purified recombinant HcpR with or without the 6x-His tag appears as a monomer or dimer on SDS-PAGE gel. The purification method yields a pure (≥95%), mono-disperse protein solution in all buffers used. When reducing agents are added to the gel loading sample nearly all of the sample exists as a monomer. The presence of a cysteine residue (C33) allows for disulfide bond formation. Treatment with TEV protease yields de-tagged HcpR, which has an apparent molecular weight of approximately 20-25 kDa.

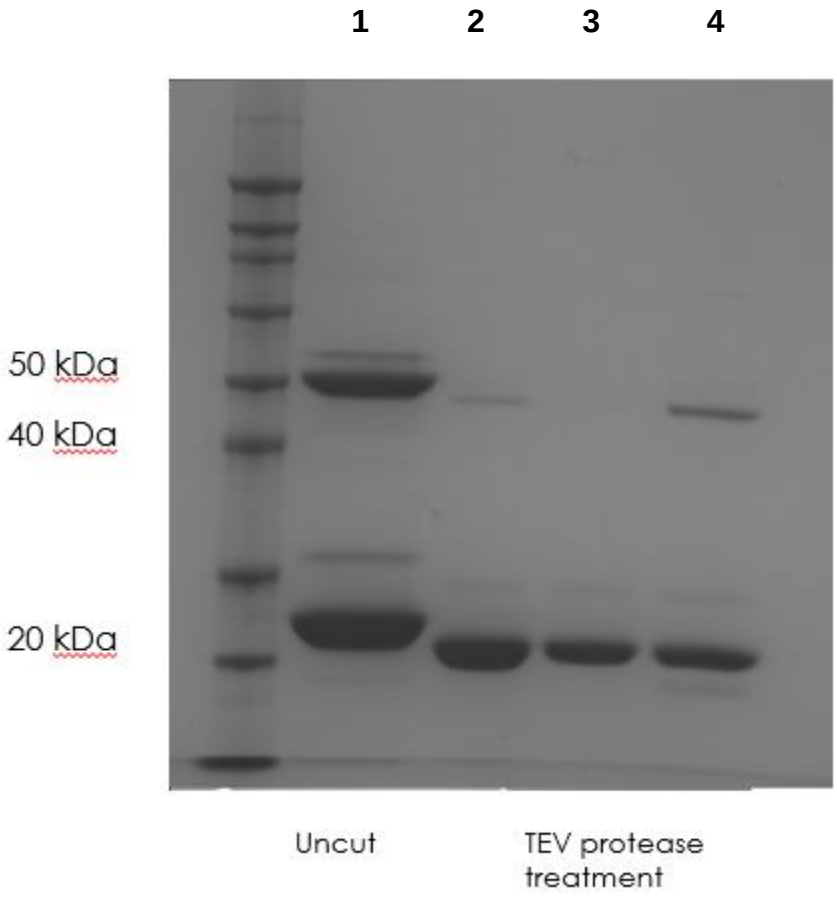

Figure 11 – SDS-PAGE gel of purified HcpR

Purified HcpR run on a 10% SDS-PAGE gel. The uncut lane (1) is run without reducing agents. After treatment with TEV protease (2-4) there is a noticeable reduction in the size of the protein.

4.3 Molecular Weight Calculation

Initial molecular weight estimation using purified recombinant tagged-HcpR from the pET30-*hcpR E. coli* on a native gel yielded a molecular weight estimation of approximately 100 kDa. This result was reinforced by SAXS studies and column chromatography using the pET30 HcpR. This would have distinguished HcpR from other FNR-CRP like regulators (and most prokaryotic regulators for that matter), however all of these experiments were carried out with a large Strep/His tag on the N-terminus of the protein from the pET30 vector. Attempts to remove the tag using enterokinase were unsuccessful forcing us to use an alternative purification method. The Halo-*hcpR* was expressed in the KRX *E. coli* strain and the protein was purified through immunoprecipitation and the tag removed via TEV protease digestion. Analytical centrifugation of the de-tagged HcpR confirmed that it exists in solution as approximately 45-50 kDa dimer (Fig. 13). This result is confirmed through column chromatography and SAXS studies of the de-tagged m-pET21-*hcpR* protein. De-tagged HcpR natively forms dimers just as other members of the FNR-CRP superfamily.

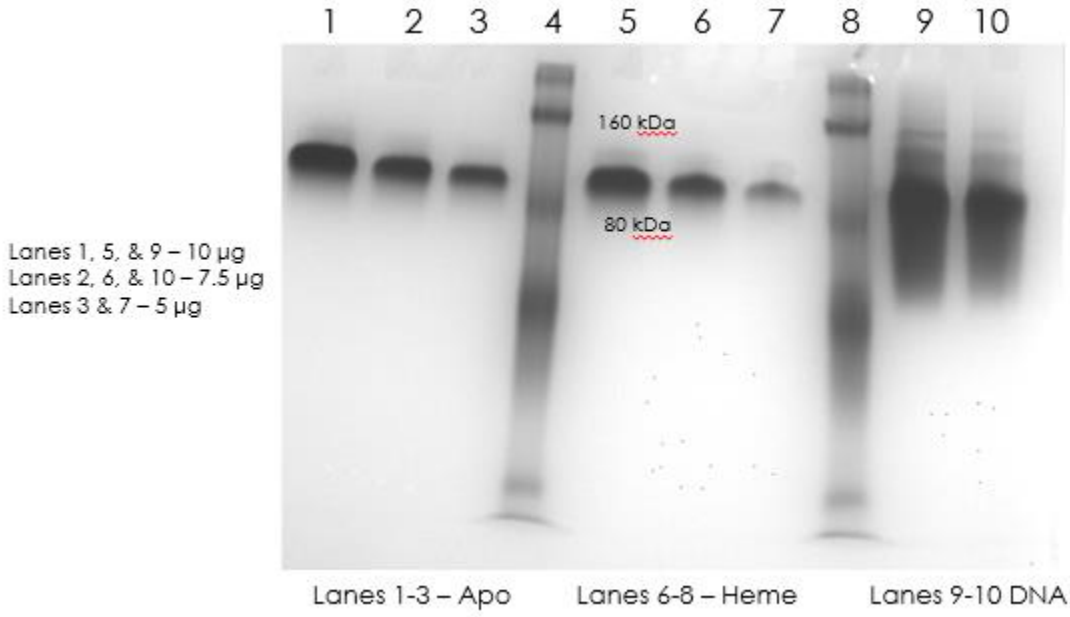

Figure 12 – Native Gel of pET30-*HcpR* protein

A Tris-Acetate native PAGE gel was used to estimate the size of the protein. Apo-HcpR (lanes 1-3), heme-HcpR (lanes 5-7), and DNA-HcpR (lanes 9-10) were run in varied concentrations. HcpR appears to be approximately 100 kDa in size in all forms of the protein.

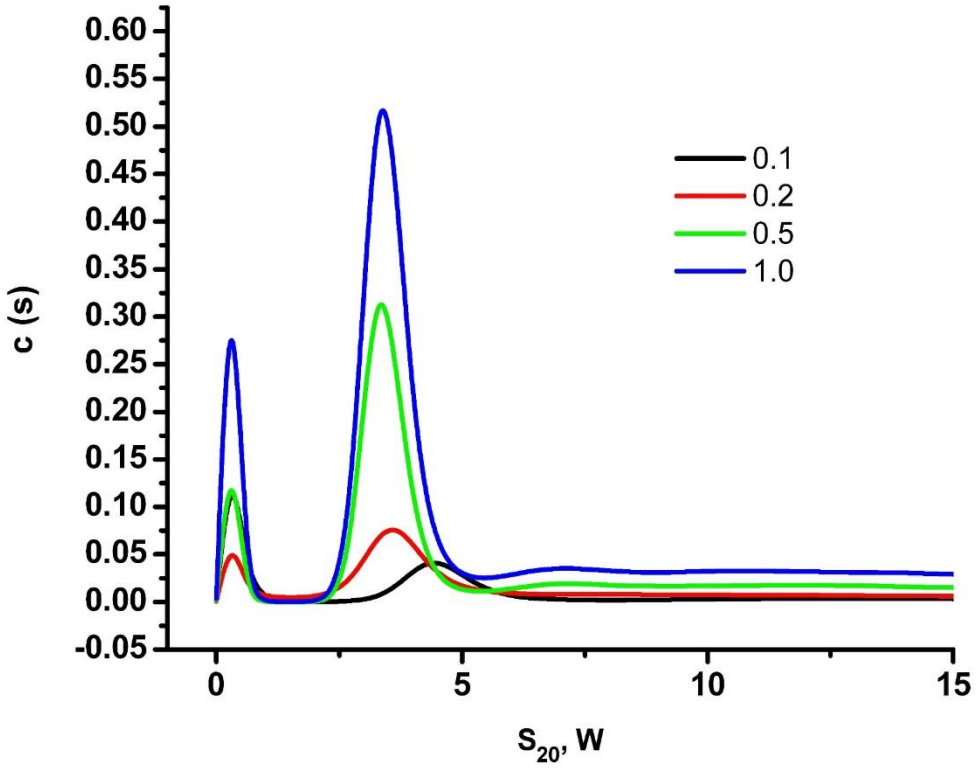

Figure 13 – Sedimentation velocity experiment of tag-less HcpR protein

Absorbance profile of the velocity experiment shows HcpR in solution as a ~48 kDa dimer. Four different concentration were used: 0.1, 0.2, 0.5, and 1.0 mg/ml. Buffer: 50 mM phosphate buffer, 150 mM NaCl, 1mM DTT.

4.4 Analysis of Heme binding

The TMBZ assay is simply a shift assay for heme and was used to initially assess the heme binding properties of HcpR (Fig. 14). Reconstituted HcpR (lane 2) was run on a native gel with positive (hemoglobin – lane 3) and negative (OxyR – lane 1) controls. After the gel ran for approximately 30 minutes it was washed and incubated with TMBZ for 15-30 minutes. The TMBZ is soaked into the gel and excess TMBZ is washed off after incubation. After washing 3% hydrogen peroxide was sprayed onto the gel. Heme has a pseudo-peroxidase activity and TMBZ is chromogenic reagent used for peroxidase detection. In the presence of peroxidase/hydrogen peroxide the colorless TMBZ will complex and form a greenish blue color. This color only forms in the regions where the heme is located. Excess heme runs to the bottom of the gel and there is a greenish stain in the middle of the gel where heme is bound to protein. This assay is not positive under denaturing conditions, HcpR must folded in a native stave to bind heme.

Circular Diochroism was used to analyze heme binding effects on secondary structure (Fig 15). With the addition of heme, there is a change in the elipticity of the sample. This corresponds to a change in the secondary structure of the protein when hemin binds. Although the addition of heme does not yield a drastic change in secondary structure, there is a small yet reproducible change in what appears to be the alpha helical nature of the protein.

The heme binding properties of HcpR were further investigated by quenching of intrinsic tryptophan fluorescence (Fig. 16).The postulated heme binding domain of HcpR has one of two tryptophan residues (W12) found in HcpR. A fluorescence time scan titration was utilized to observe the effect of heme binding in real time. Titration of heme

into Apo-HcpR resulted in a dose-dependent progressive and saturable quenching of the tryptophan fluorescence. The loss of fluorescence intensity corresponds with the addition of heme to the cuvette. A binding event occurs when heme accesses the binding pocket and this binding event causes quenching of the tryptophan residue (whether this is due to direct interaction between heme and tryptophan or the exposure tryptophan side chain to solvent is not known). This change in fluorescence intensity corresponds with binding of ligand, and will allow us to possibly ascertain the binding parameters.

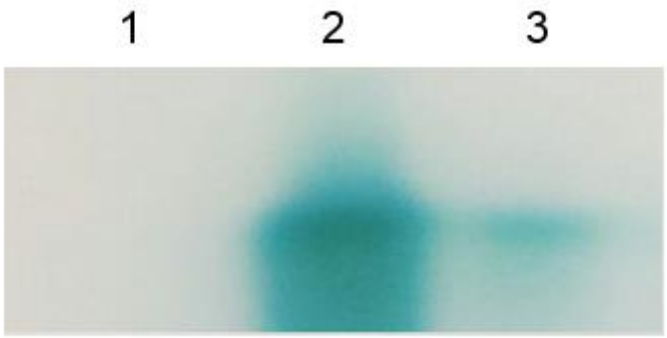

Figure 14 – TMBZ assay for heme binding

Lane 1: Negative control (*P.g.*OxyR); Lane 2: HcpR; Lane 3: Positive control (hemoglobin). Samples were run on a 12% Tris-Acetate native gel.

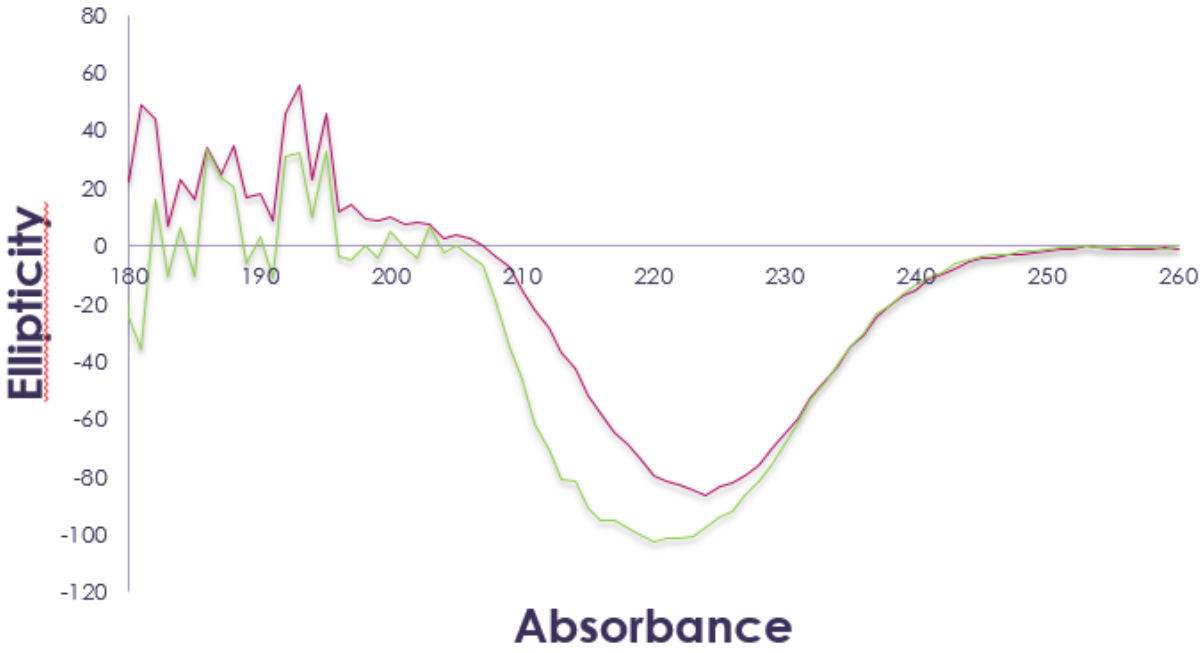

Figure 15 – CD spectra of Apo- and Heme-HcpR under

Dark: Apo-HcpR at 0.15 mg/mL Light: Heme-HcpR at 0.15 mg/mL.

Heme binding assayed using CD spectroscopy. Binding of heme causes a reproducible shift in the elipticity caused by a change in the secondary structure.

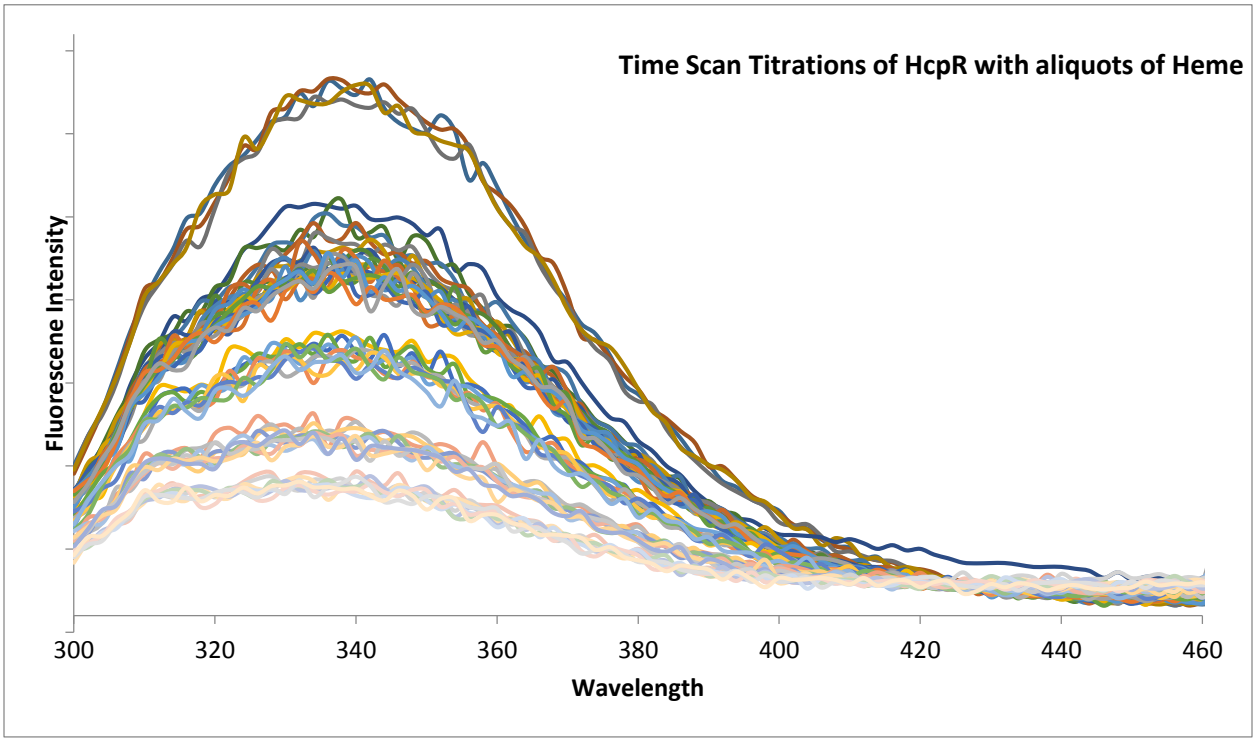

Figure 16 – Heme Time scan titration of HcpR

HcpR was titrated 4 times with 5 µg of heme to a 5 mM solution and excited at 280 nm. A time scan titration of the mixture over a spectrum of 300-460 nm. After the addition of heme to the sample there is a noticeable and reproducible decrease in the fluorescence intensity.

The UV-Vis spectrum of HcpR-heme dilution series under aerobic conditions is shown in Figure 17. There appears to be no dose dependent change in the spectrum due to heme binding. This is unexpected as most heme binding proteins will show a change in the soret region (~400 nm) upon addition of heme to the binding site. No soret peak appears in any concentration. This issue is resolved when addition of heme is done under anaerobic conditions (Fig. 18). As can be clearly seen, a very sharp soret peak appears at 394 nm when the heme is added under anaerobic conditions. This effect is reproducible and is seen in the NO binding studies also.

To further quantify the heme binding properties of HcpR, a dilution series of heme was measured for their intensities, while keeping the concentration of HcpR constant (Table 3). The data points were used to construct a binding curve, from which the K_d can be approximated (Fig. 19). The result yielded a value of K_d = 155.6 µM. This value is extremely high and indicates relatively weak binding of heme to HcpR.

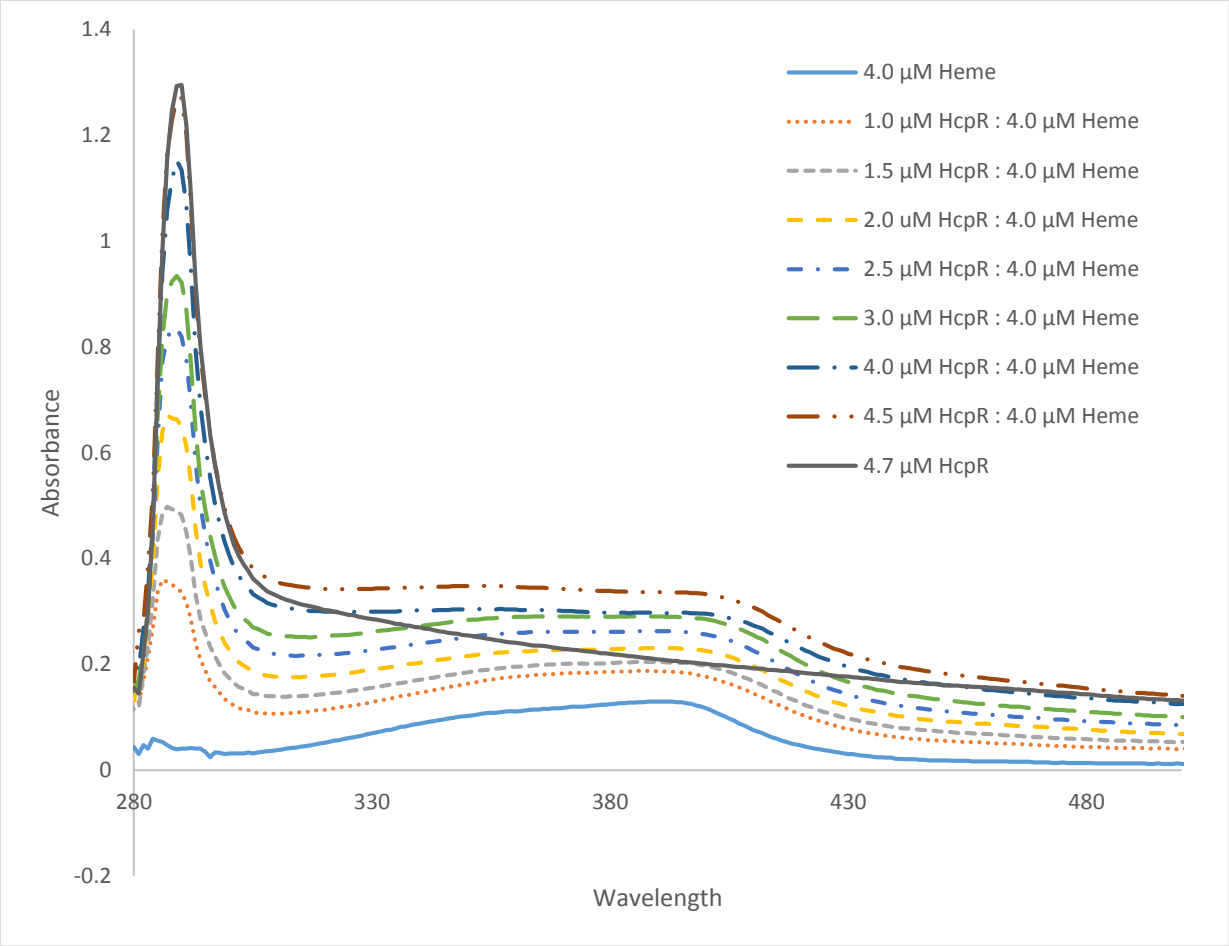

Figure 17 – Affinity of HcpR for heme under aerobic conditions

The affinity of HcpR for heme was tested using UV-Vis spectroscopy. All experiments were done aerobically. Different molar ratios were tested and binding was monitored over a range of 280-500 nm. There seems to be no change in the morphology of the spectrum due to changes in the protein concentration. However, there is an increase in the absorbance due to the increase of protein concentration.

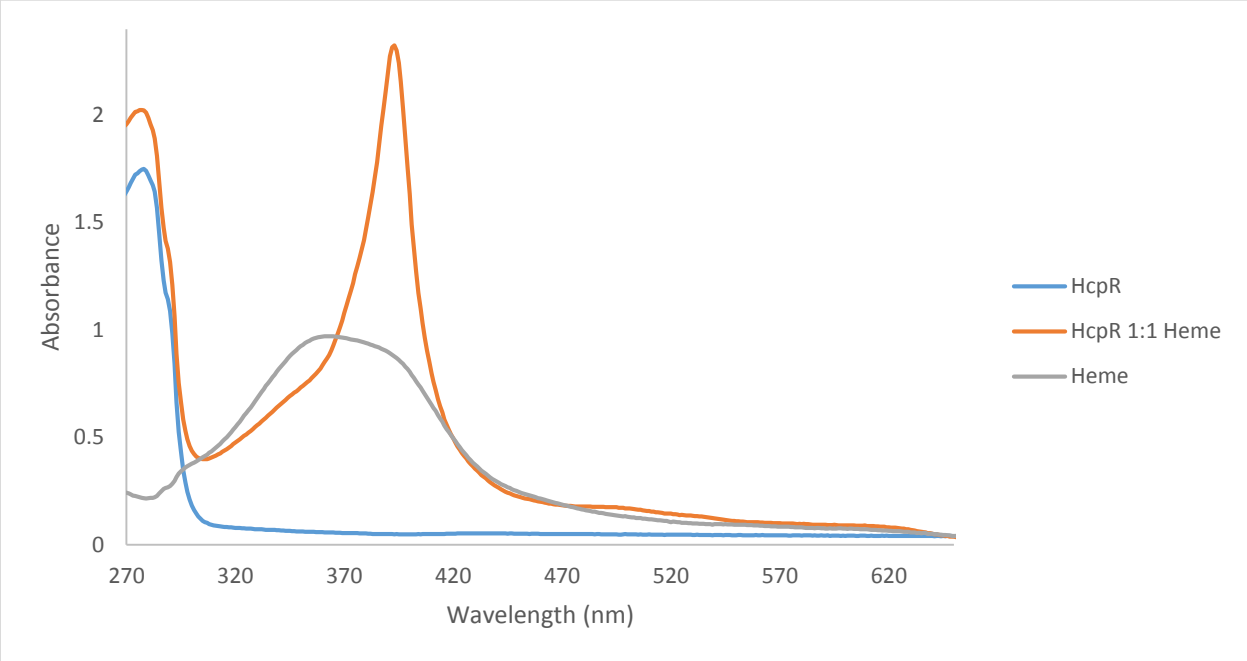

Figure 18 – UV-Vis spectrum of Heme binding under anaerobic conditions

Heme (Fe^{2+}) binding was analyzed under anaerobic conditions. A 1:1 ratio of heme to HcpR forms a large Soret peak at 398 nm.

Table 3 – Measurement of Heme to HcpR binding through intrinsic HcpR fluorescence quenching.

HcpR concentration was held constant at 6.667 μM and heme titrated from 0 μM – 542 μM heme. The intrinsic fluorescence intensity of HcpR was measured. Sample was excited at 280 nm and emission was measured at 340 nm.

Heme Concentration	Relative Intensity
0 μM	130.1341
28μM	105.4234
40μM	92.93639
76 μM	86.01876
112 μM	81.88692
148 μM	69.70366
170 μM	65.19112
222 μM	53.59291
364 μM	22.22325
470 μM	15.37927
542 μM	11.2592

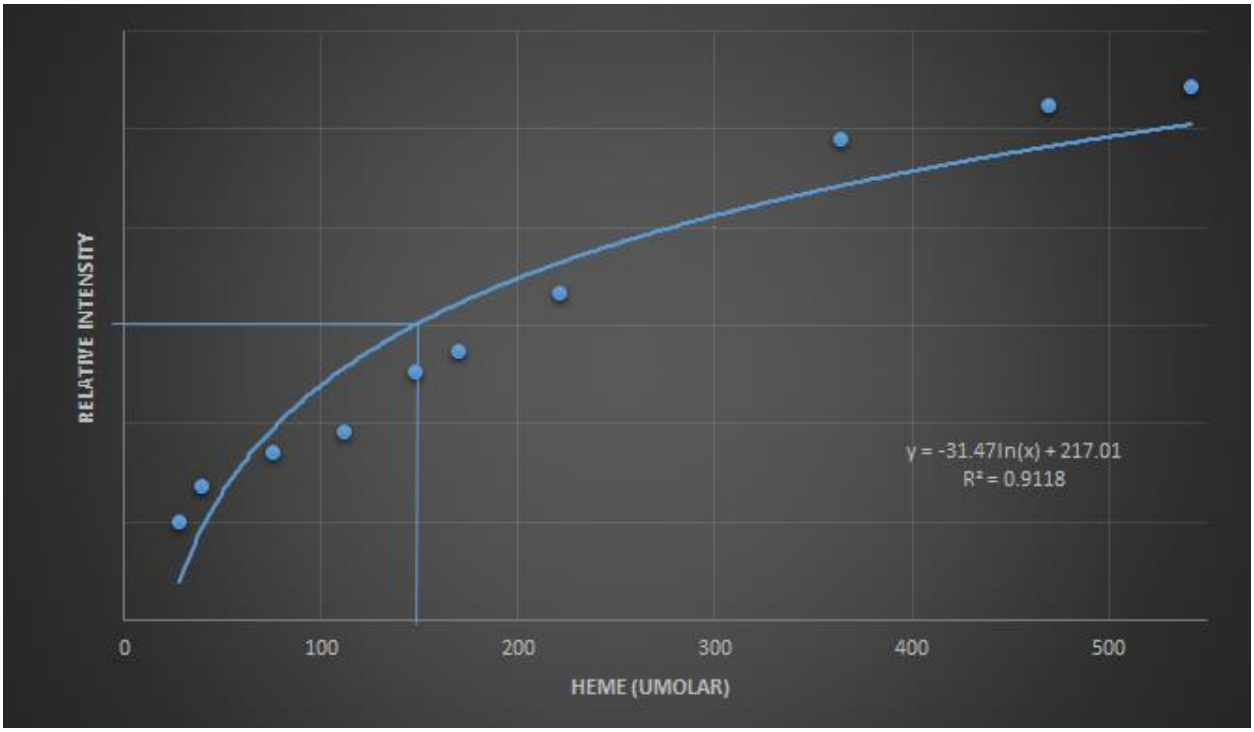

Figure 19 – Affinity of HcpR to heme – fluorescence generated titration binding curve.

Heme dilution series was plotted and fit to a logarithmic curve. At 0.5 occupancy that substrate concentration is equivalent to the K_d. This yielded a K_d value of approximately 155.6 µM

4.5 Analysis of NO binding

Figure 20 shows the spectral properties of heme reconstituted and reduced HcpR under anaerobic conditions before and after the addition of nitric oxide. The reduced sample displays a very sharp Soret peak at 392 nm that has a shoulder at 350 nm. Upon the addition of NO the peak remains ~392 however the shoulder at 350 nm is not retained. There is also a slight but reproducible shift in the peak at 620 to 569 upon the addition of NO.

Resonance Raman spectroscopy further elucidated the properties of NO binding to HcpR. A series of resonance Raman spectra of the sample before and after the addition of NO is displayed in Figure 21. The polarization and depolarization components are also displayed. Among other characteristics of the graph, the most prominent is the shift at the 1362 cm^{-1} position to 1376 cm^{-1} position after addition of NO. Designated as the ν_4 band, these regions have been shown to be sensitive to XO binding in other heme proteins. Other vibrational markers appear as well, ν_3 at 1508 cm^{-1}, ν_2 at 1584 cm^{-1} and ν_{10} at 1646 cm^{-1}. The peaks in these regions have been shown to be characteristic of NO binding in cytochrome c and hemoglobin (Spiro, Strekas 1974, Andrew, Green et al. 2001). Furthermore, these would indicate that there is a 5 coordination binding of NO to a ferrous heme. In the low frequency region, the appearance of a peak at the 535 cm^{-1} region is most likely the ν(Fe-NO) mode. This frequency is in the expected range for a 5 coordinate Fe(II)NO heme, as opposed to a 6 coordinate Fe(II)NO heme which gives a frequency closer to 550 cm^{-1} (Tomita, Hirota et al. 1999). The change in peak intensity at the 756 cm^{-1} region has been shown to change in the binding of NO to cytochrome c.

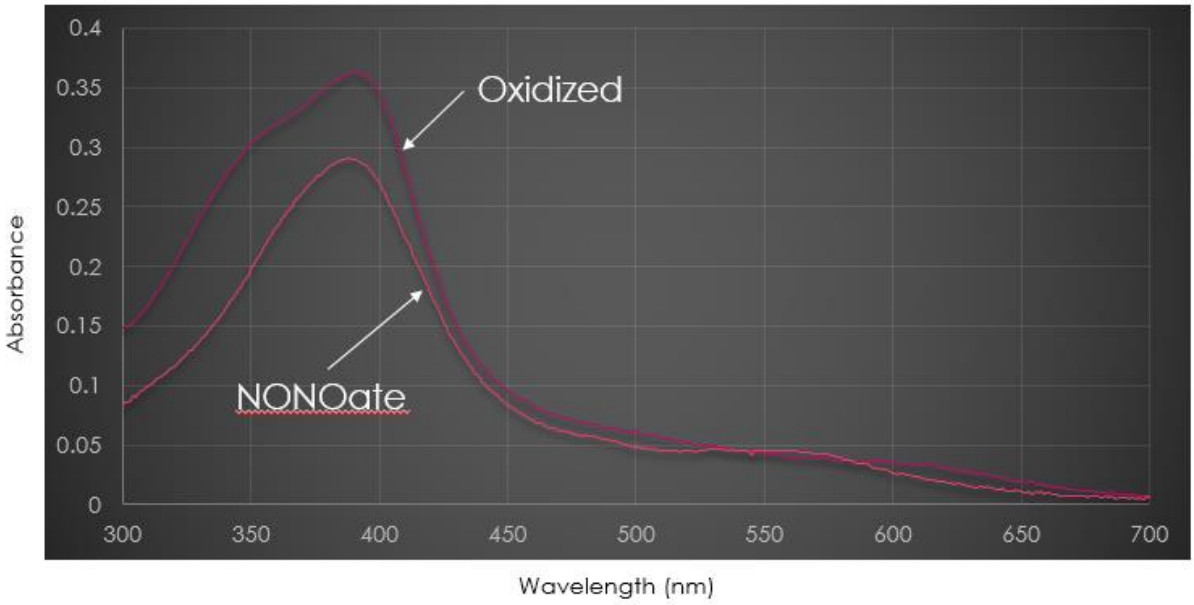

Figure 20 – Anaerobic UV-Vis spectrum of HcpR – with NO.

Reconstituted HcpR was reduced using dithionite and scanned from 300-700 nm to yield Fe^{3+} HcpR (oxidized line). NONOate was used to produce an excess of NO. The reduced sample was then incubated with an excess of NO (NONOate line). Addition of NO yields a species with a similar profile to the Fe^{2+} heme.

A

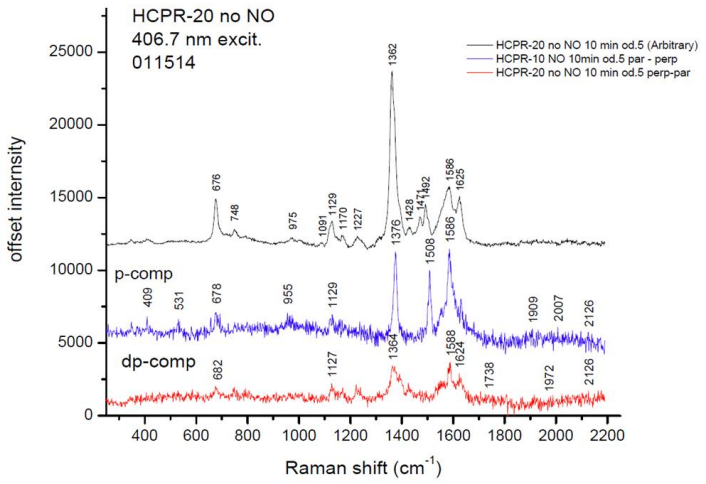

B

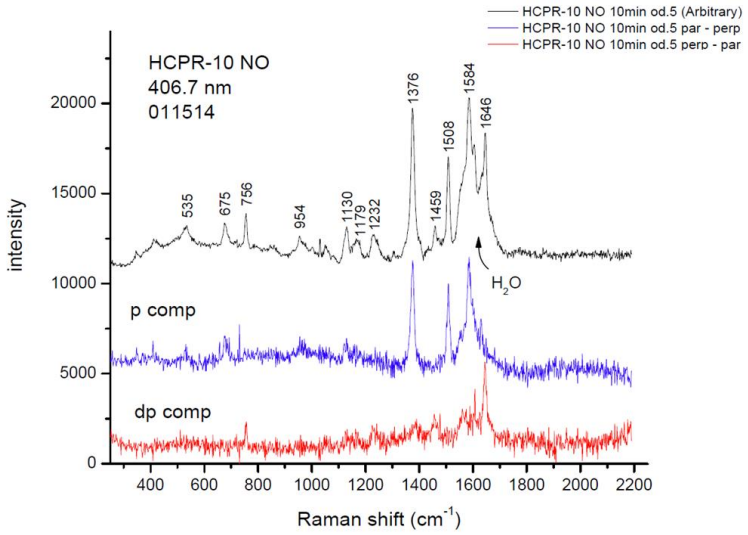

Figure 21 – Resonance Raman Spectrum of HcpR

Reconstituted HcpR was incubated with dithionite under anaerobic conditions. The Raman spectrum was generated under anaerobic conditions. The nitrosylated sample was generated using an excess of NONOate dissolved in buffer and added to the sample. Panel A – HcpR without NO; Panel B – HcpR with NO added

4.6 Structural analysis of HcpR with Small Angle X-ray Scattering

Table 4 shows the structural parameters of the different forms of HcpR as determined by SAXS experiments. Figures 22-24 shows the scattering profiles log I(q) vs. S and Guinier plots (inset) for the Apo-, heme-, and DNA- form of the protein. The scattering profile for each form of HcpR shows a typical profile of a globular protein with a cylindrical shape. The Apo-HcpR sample shows a pure, mono-disperse sample with no aggregation. However, in the Heme-HcpR sample there is evidence in the scattering profile that the aggregation is occurring. Guinier analysis of the scattering data for the Apo-HcpR gives an expected linear fit for a pure, monodisperse solution and yields a radius of gyration (R_g) of 27.65 ± 0.02 for the Apo form of the protein. This also is evident in the Kratky plots (Fig. 25). The Kratky plots are a good estimate of the overall stability and integrity of the sample. A completely folded protein will form a curve shape on the graph and a completely unfolded sample will have a logarithmic shaped graph. As can be seen in the samples, the Apo and DNA forms of HcpR appear to be in a fully folded state, however, the heme form appears to be partially unfolded. This is not unexpected as the heme HcpR has had stability and precipitation problems.

The distance distribution functions were calculated using GNOM (Fig. 26) and shows the Apo form of the protein has a max diameter (D_{max}) of approximately 83.1 angstroms. The D_{max} of the heme- and DNA- forms of the protein increases, however, the data from these samples is inconclusive. The stability and integrity of the protein is brought into question and aggregation issues were evident in the heme form of the sample.

The D_{max} and R_g of the Apo-HcpR suggests that HcpR is a longer, more cylindrical protein, as is predicted in the homology model. Furthermore, the molecular mass determination using Autoporod reveals that the molecular weight is approximately 47 kDa. To compare the HcpR homology model with the SAXS data more in depth, the FoXs server was used to construct a theoretical scattering profile of the model (Fig 27). A theoretical curve of the monomer and dimer form of the model was generated. As can be seen, the dimer homology model theoretical scattering profile overlays very well with the Apo-HcpR scattering profile which supports previous data.

The *ab initio* reconstructed models were generated using DAMMIF and the GNOM log file. Ten models of each form of the protein were created and then clustered and scored; the best scoring model from the highest populated cluster was chosen. The models were constructed out of dummy residues in UCSF Chimera. As can be clearly seen in Figure 28, the shape of the Apo-HcpR *ab initio* model is comparable to the shape of the HcpR homology model. However there are clear differences: the N-terminal heme binding domain appears to be more “stretched” in the *ab initio* model and more compact in the homology model. The heme-HcpR and DNA-HcpR *ab initio* models (Fig. 29-30) are not as well organized as the Apo-HcpR *ab initio* model. This is an expected result, given the partially unfolded state of the protein and the aggregation problems in the presence of heme.

Table 4 – Structural parameters from SAXS data

	Apo-HcpR	**Heme-HcpR**	**DNA-HcpR**
R_g	28.2 ± 0.15	29.3 ± 0.2	31.2 ± 0.2
D_{max}	94.5 Å	95.96Å	109.2 Å
I(0) (from Guinier)	63.36	76.5	138.6
I(0) (from P(r))	63.89	78.5	136.4
M.W.	47 kDa		

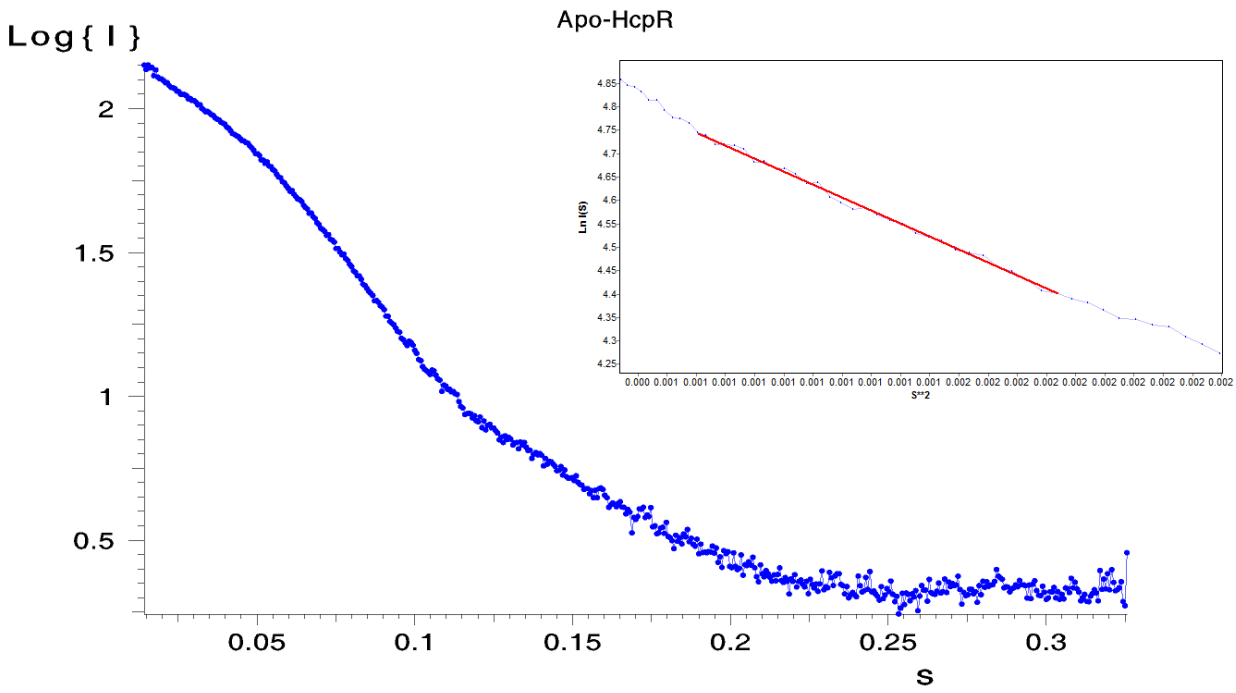

Figure 22 – SAXS Scattering profile and Guinier plot for Apo-HcpR

Scattering profile of the Apo-HcpR sample generated from merging samples of a same concentration. Inset shows the Guinier plot and associated linear fit (solid line) of the data in the Guinier region.

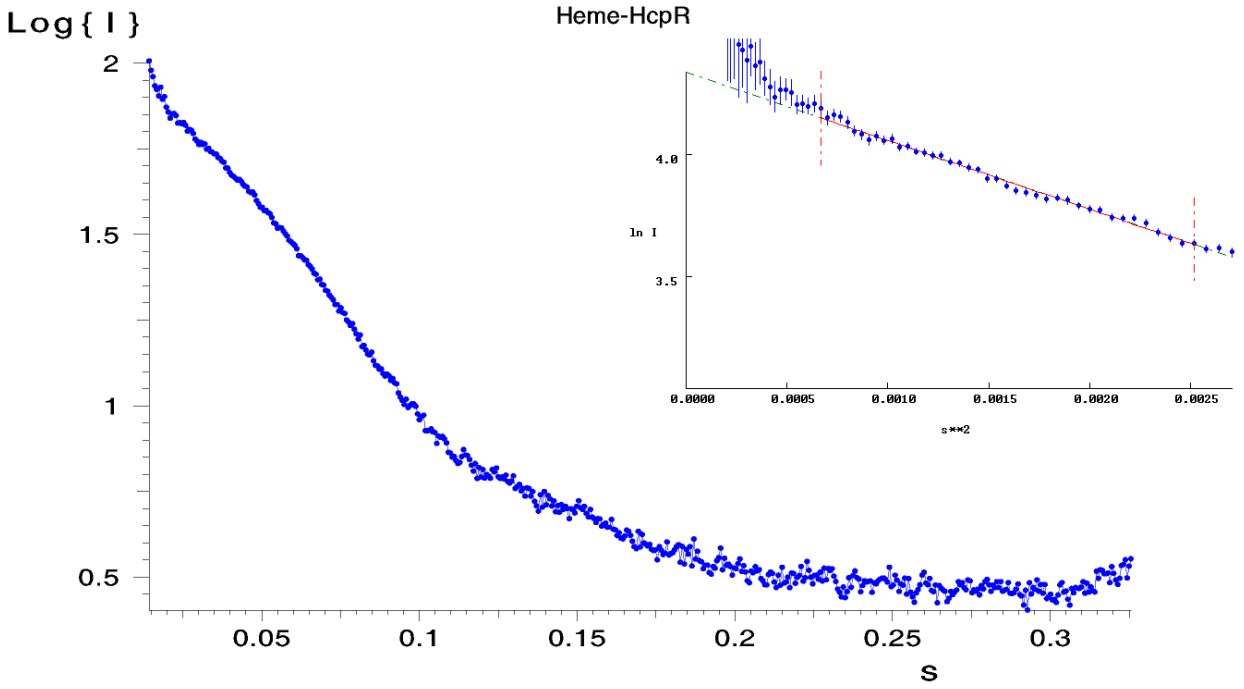

Figure 23 – Scattering profile and Guinier plot for Heme-HcpR

Scattering profile of the heme-HcpR sample generated from merging samples of a same concentration. Inset shows the Guinier plot and associated linear fit (solid line) of the data in the Guinier region.

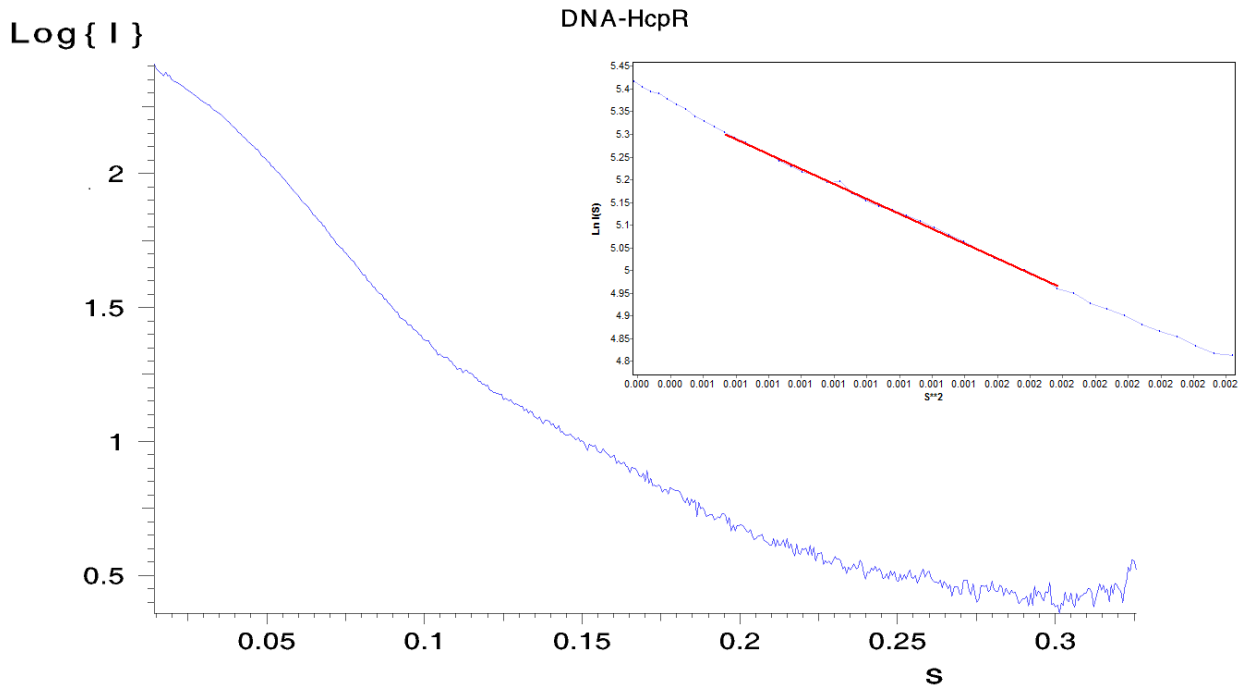

Figure 24 – Scattering profile and Guinier plot for DNA-HcpR

Scattering profile of the DNA-HcpR sample generated from merging samples of a same concentration. Inset shows the Guinier plot and associated linear fit (solid line) of the data in the Guinier region.

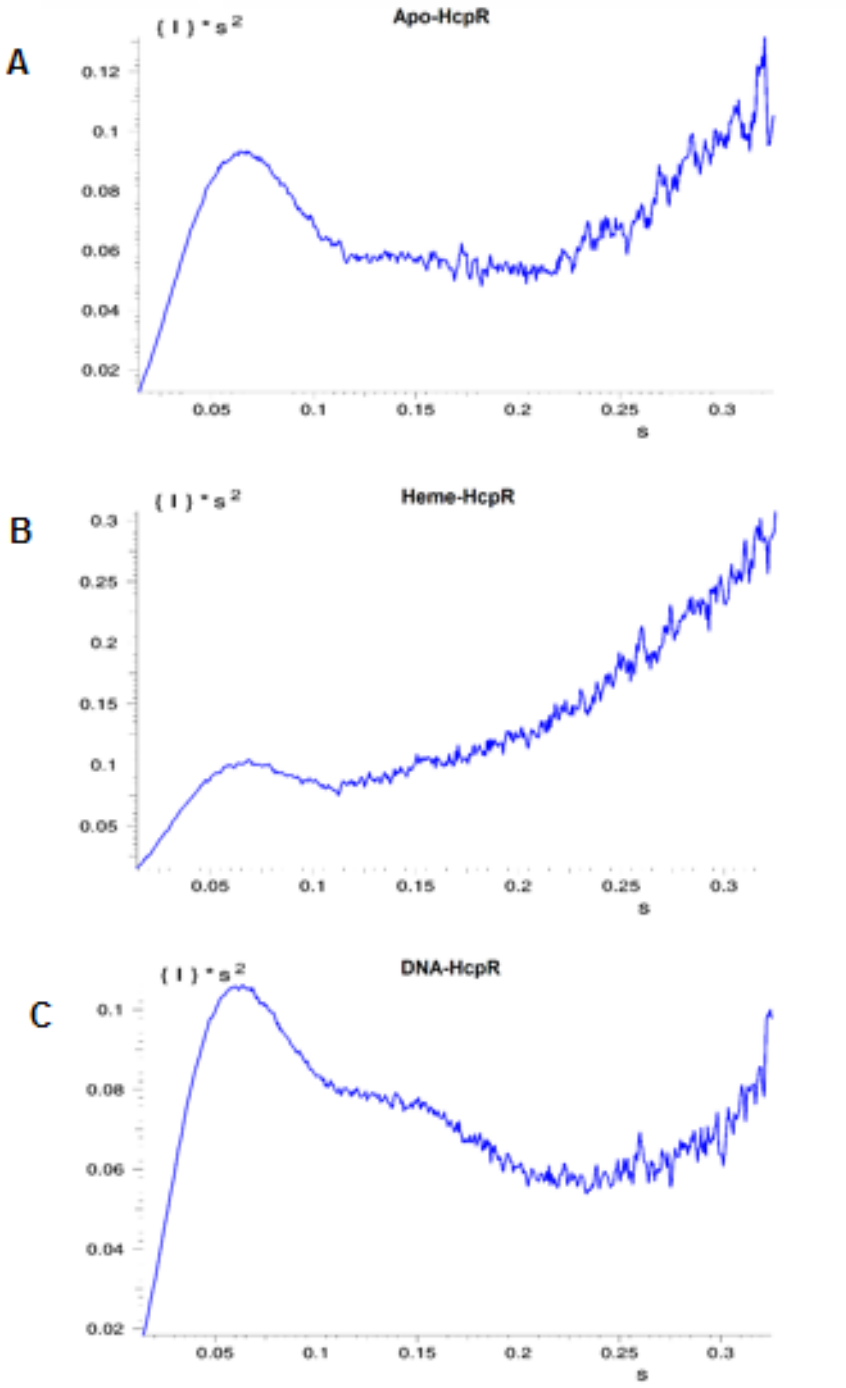

Figure 25 – Kratky plots for HcpR

Kratky plots derived from Figures 22-24 to test the protein stability and folded state of 3 forms of HcpR: Apo-HcpR (**A**), Heme-HcpR (**B**), DNA-HcpR (**C**). The Kratky plot of the Apo-HcpR protein is characteristic of a globular protein.

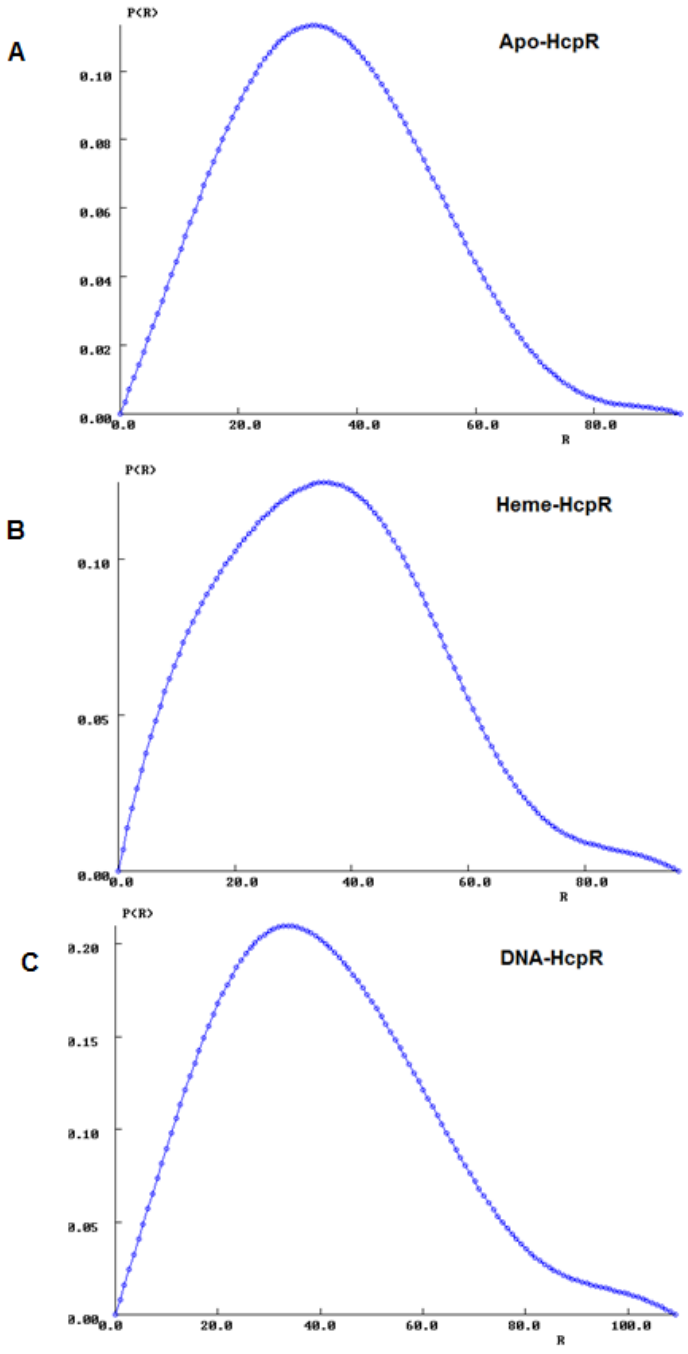

Figure 26 – Distance Distribution functions P(r)

The P(r) profiles for the different forms of HcpR: Apo-HcpR (**A**), Heme-HcpR (**B**), DNA-HcpR (**C**). The profile for each form of HcpR was generated using a Dmax value calculated using the program DATGNOM, and is listed in Table 4

A

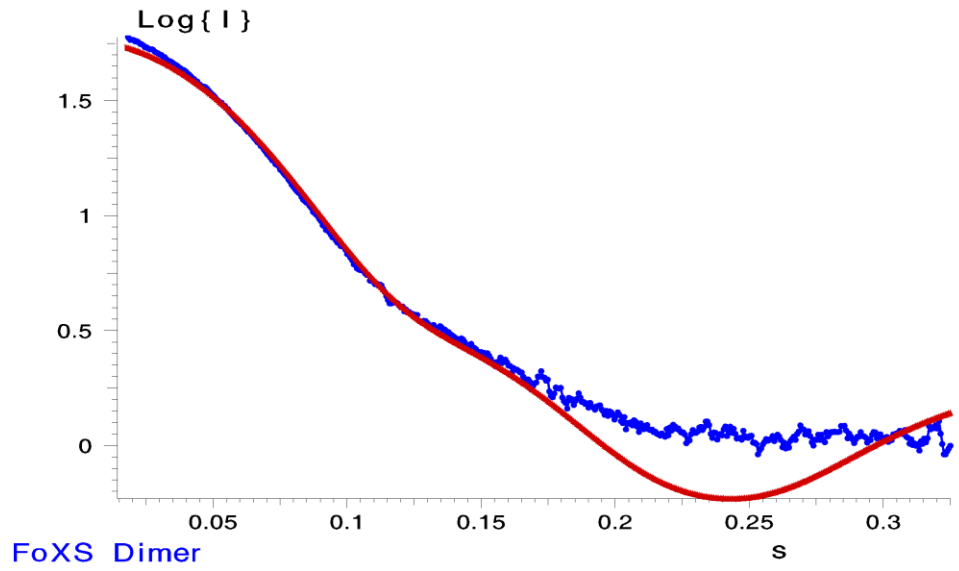

B

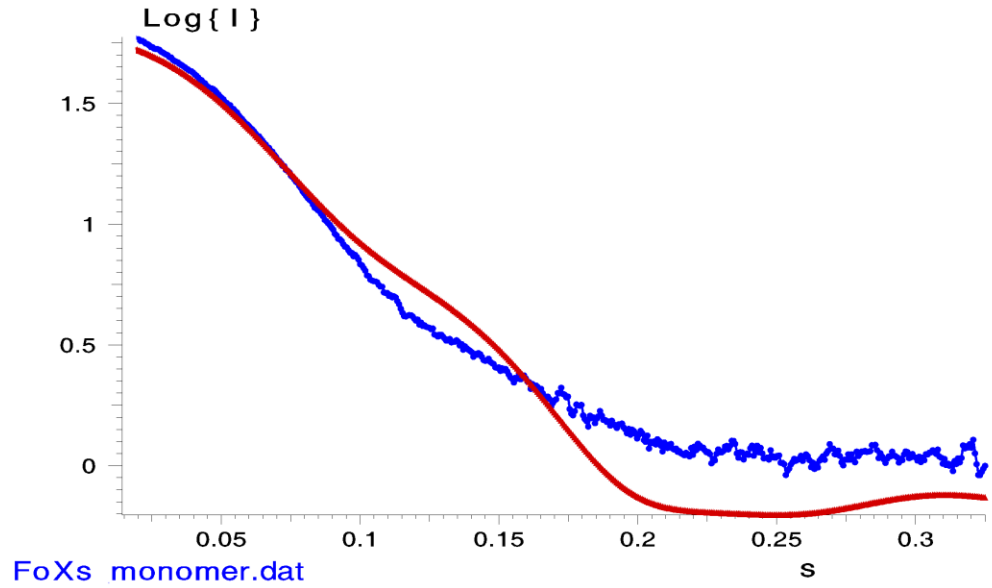

Figure 27 – Comparison to theoretical scattering profiles

Theoretical scattering profile of dimer (**A**) and monomer (**B**) of Apo-HcpR homology models over-layed with Apo HcpR scatting profile. Theoretical profiles generated using the FoXs server.

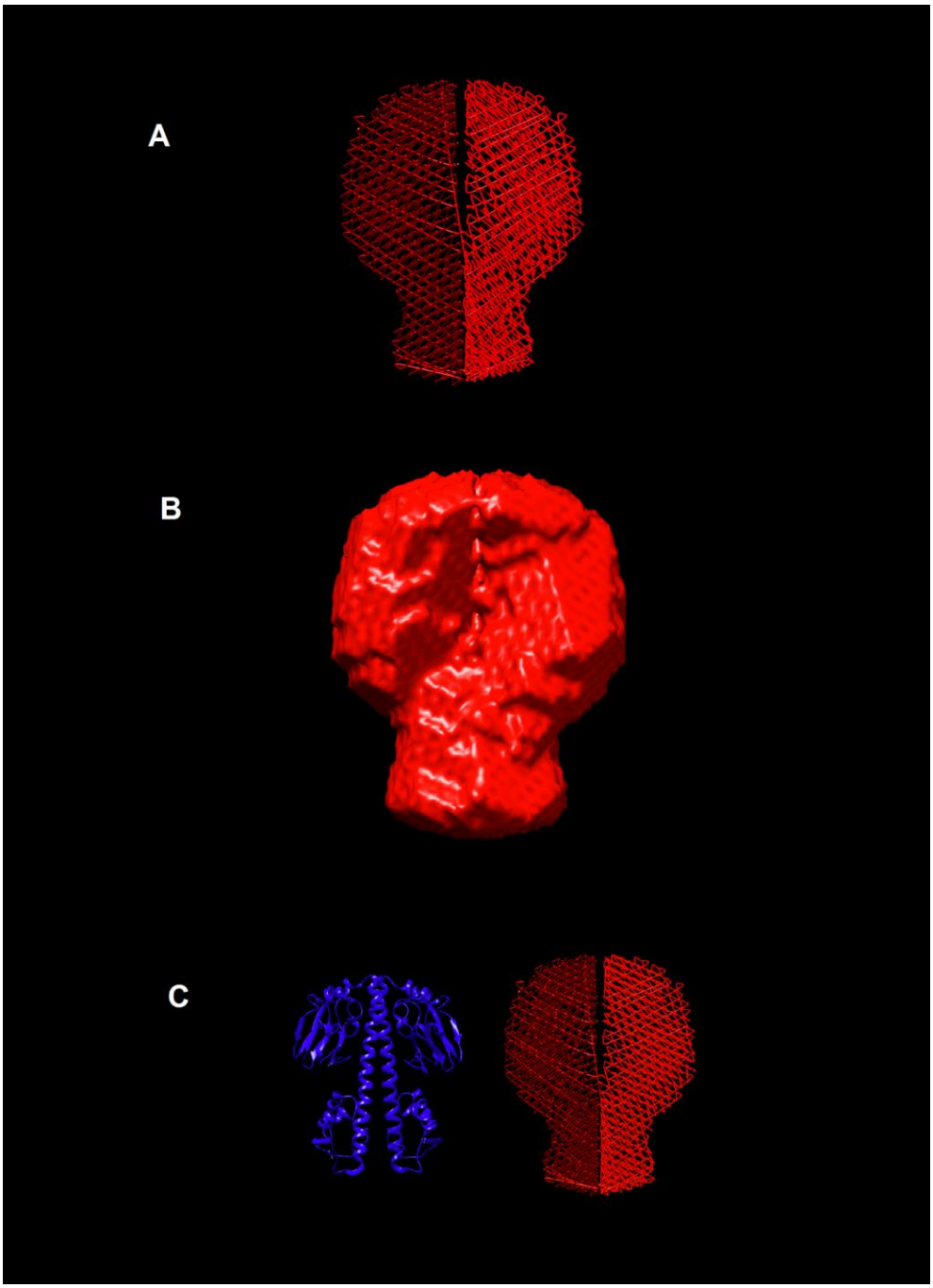

Figure 28 – *ab initio* model of Apo-HcpR

The *ab initio* shape reconstruction of Apo-HcpR, calculated from the scattering data, generated by DAMMIF. The models are represented using dummy atoms (**A**) and volume reconstruction (**B**). The HcpR homology model is compared to the *ab initio* dummy atom model (**C**).

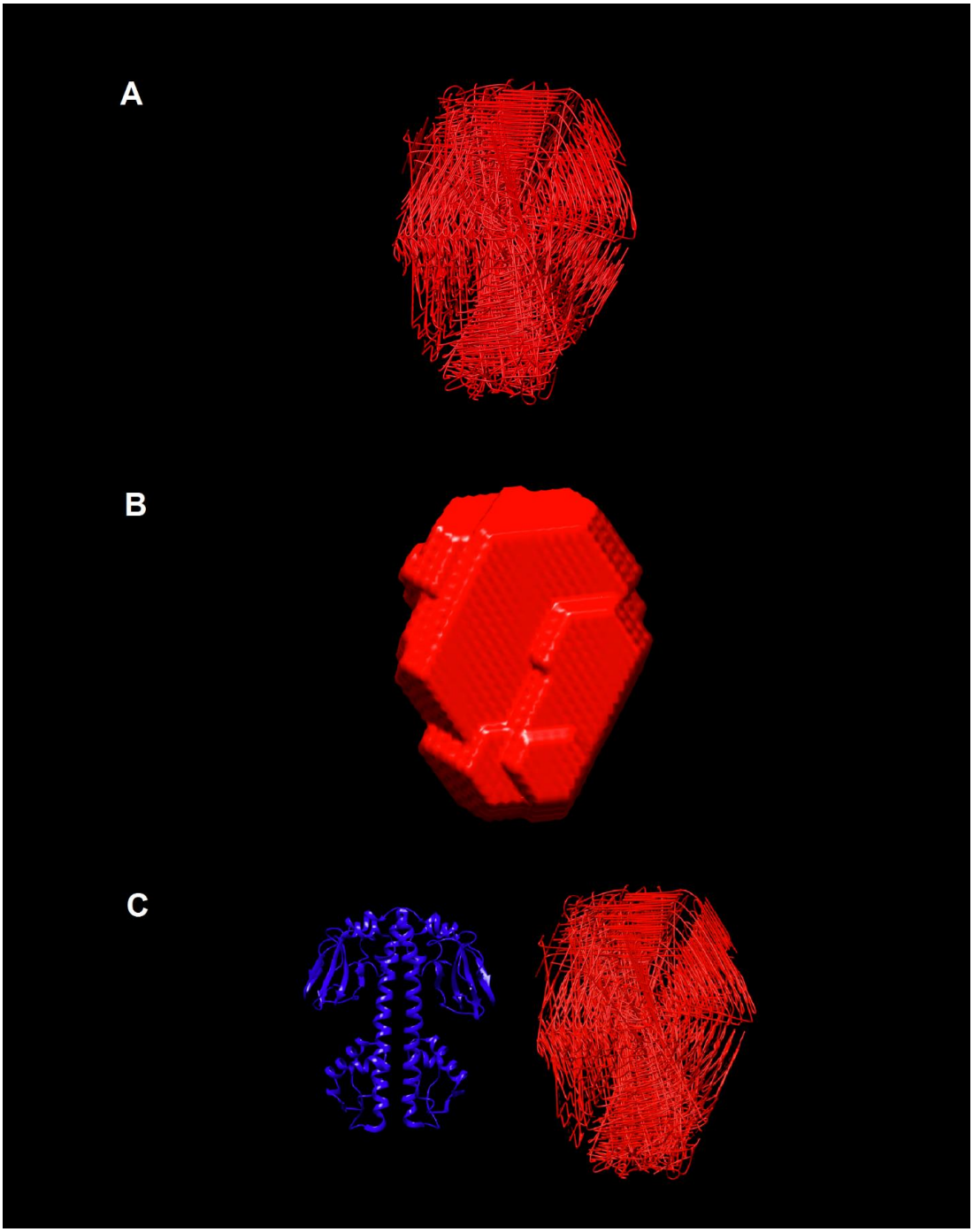

Figure 29 – *ab initio* model of Heme-HcpR

The *ab initio* shape reconstruction of Heme-HcpR, calculated from the scattering data, generated by DAMMIF. The models are represented using dummy atoms (top) and volume reconstruction (middle). The HcpR homology model is compared to the *ab initio* dummy atom model (bottom).

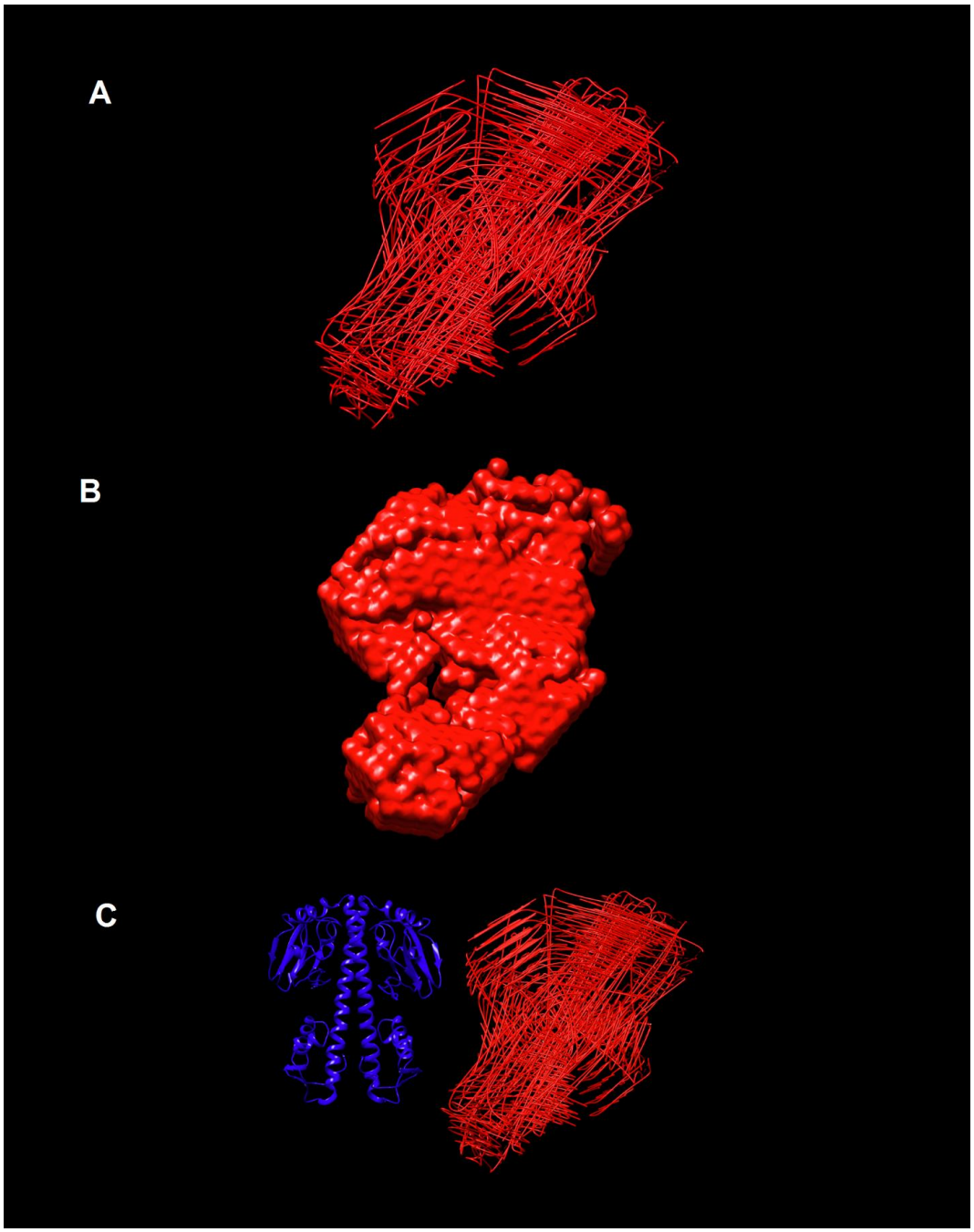

Figure 30 – *ab initio* model of DNA-HcpR

The *ab initio* shape reconstruction of DNA-HcpR, calculated from the scattering data, generated by DAMMIF. The models are represented using dummy atoms (**A**) and volume reconstruction (**B**). The HcpR homology model is compared to the *ab initio* dummy atom model (**C**).

4.7 Promoter studies

There is no change in fluorescence when the bacteria are exposed to a testing range of 1 μM – 20 μM NONOate or nitrite for one hour. The basal level of expression of the P-glow gene was observed in TOP10 *E. coli* (Fig. 32). The P-Glow-BS2 plasmid contains a constitutive promoter. The PA-glow and PG-glow vector express very low amounts of the fluorescence protein. The P. Glow-Bs2 vector has a constitutive *E. coli* promoter upstream of the glow gene, causing a low basal expression of the fluorescent protein.

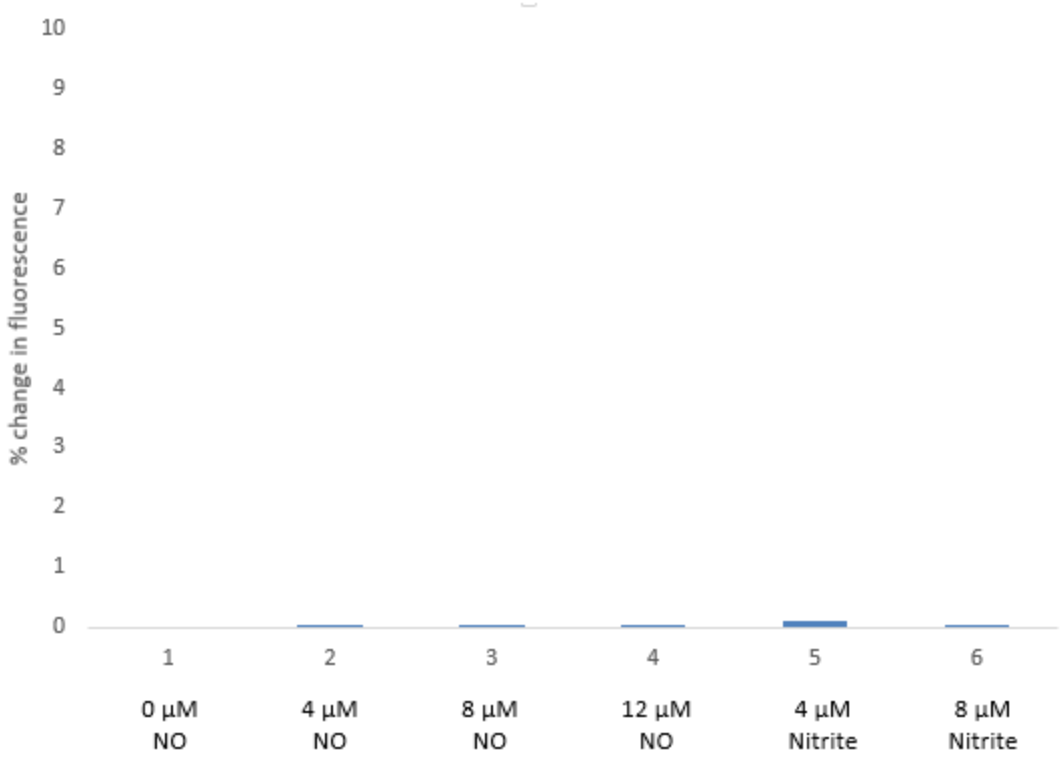

Figure 31 – NO and Nitrite stimulated activation of the *hcp* promoter by HcpR in *E. coli.*

NO and nitrite dependent activation of the *hcp* promoter was measured using the BS2 fluorescence reporter gene. The PG-glow vector and pACYC-*hcpR* vector were expressed simultaneously in *E. coli* and grown anaerobically in nitrites. The fluorescence was measured using a fluorescent plate reader.

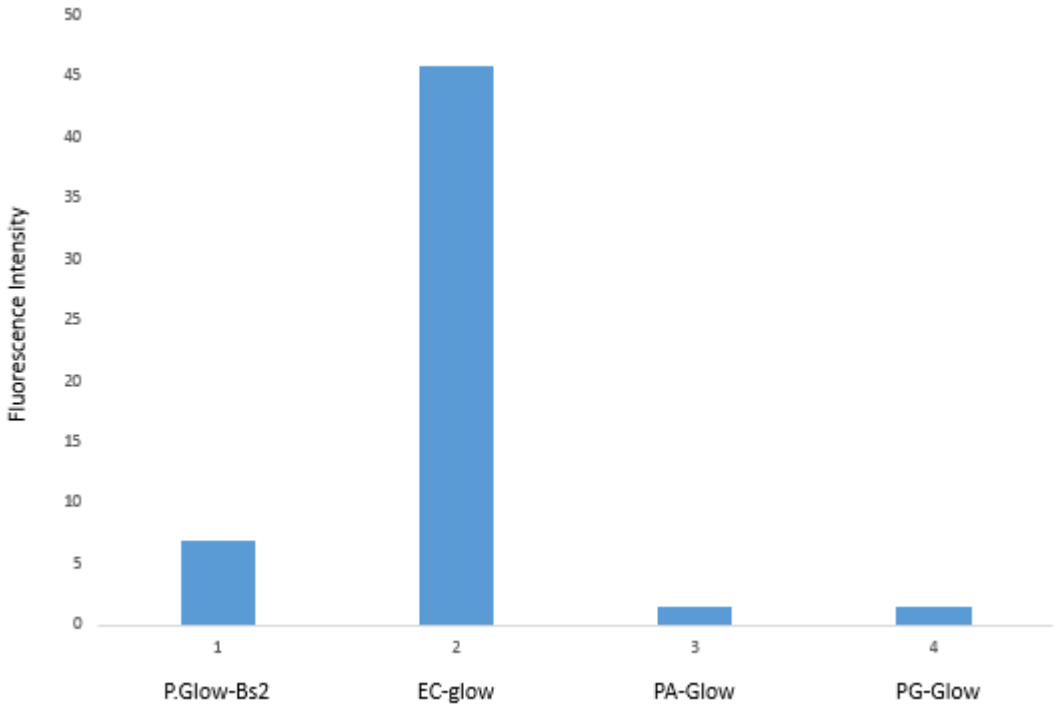

Figure 32 – Base level expression of fluorescent reporter gene for different constructs

Each construct was transformed into *E. coli* and grown anaerobically. The basal expression level of the fluorescent BS2 reporter gene was measured in each strain using a fluorescence plate reader. The P-glow-BS2 vector contains a constitutive *E. coli* promoter that has low basal level expression.

4.8 Crystallization of HcpR

After screening conditions, crystals of HcpR were obtained by oil drop diffusion method by combining 2 uL of protein solution (10 mg/mL protein in 100 mM NaCl, 25 mM TRIS-HCl, 1 mM TCEP, pH 7.5) with 2 uL of screening solution (6% PEG 8k, 100mM TRIS pH 8.0). The crystal grew in approximately 1 month with a rhombohedral shape. Cryo used was the mother liquor with 30% Glycerol added.

Crystal belongs to P orthorhombic crystal system. The unit cell parameters are: a= 93.23, b=129.41, c=150.52 A. May be 2 dimer (4 monomer) per asymmetric unit with water content approximately 72%.

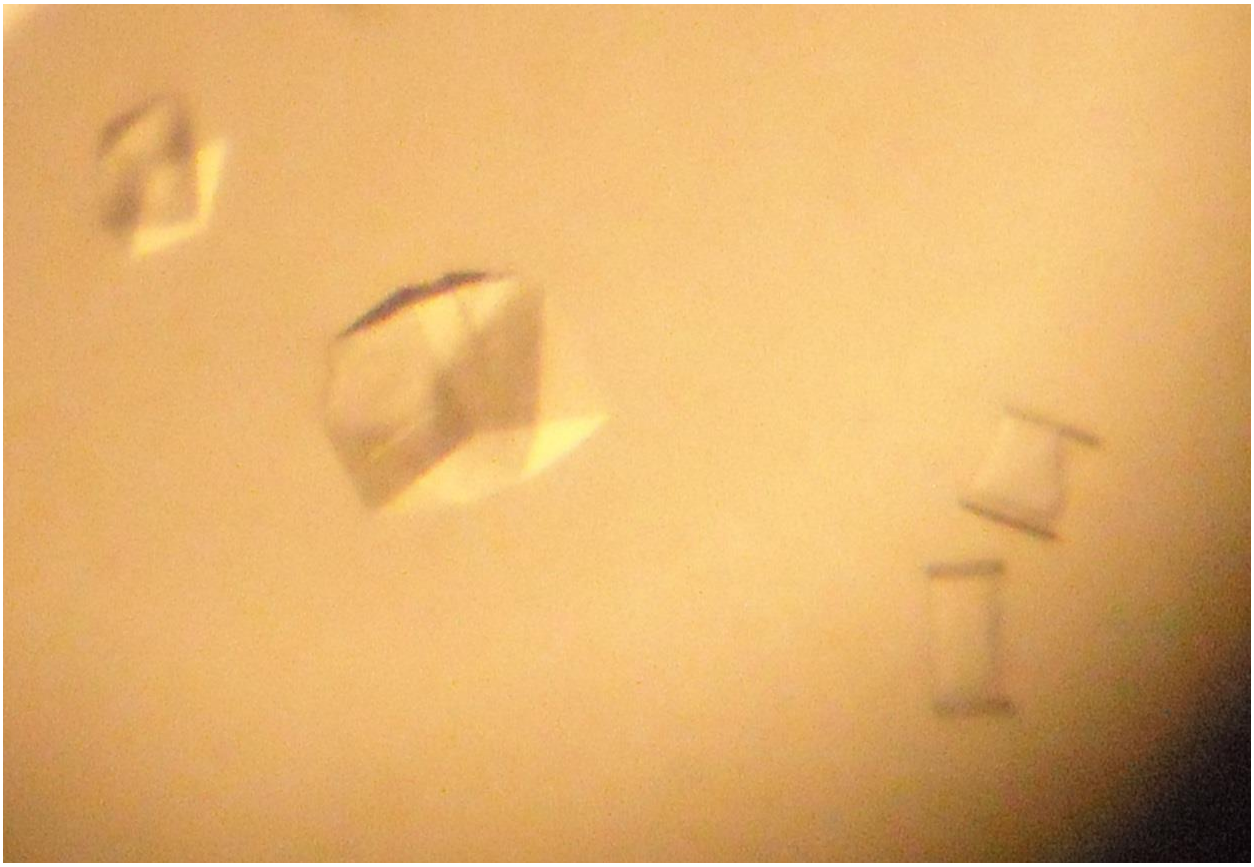

Figure 33 – HcpR Crystals from screening.

Native, full length HcpR crystals grown at 20 mg/ml concentration in a 6% PEG 8k, 100mM TRIS pH 8.0 solution. Crystals are 3-dimensional and orthorhombic in shape.

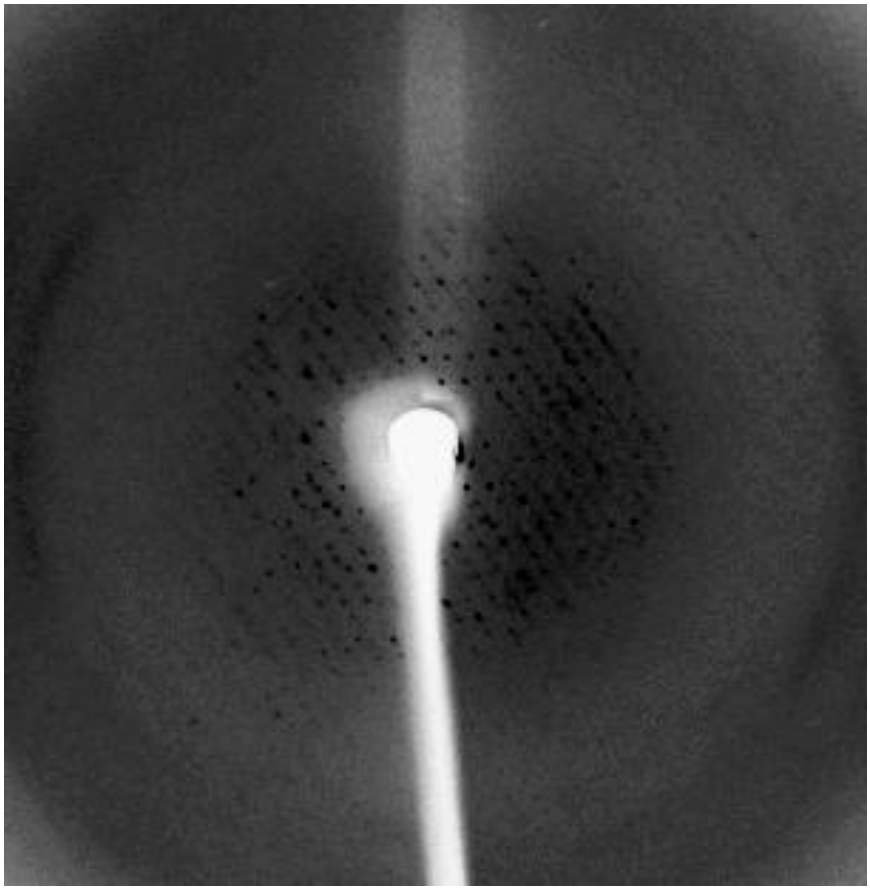

Figure 34 – HcpR Crystal diffraction pattern

Diffraction pattern generated from the above (Fig. 33) crystals. Cryoprotectant used for crystals was 30% glycerol. Resolution of diffraction is 8-10 Angstroms.

Chapter 5 – Discussion

The nitrosative stress response is not well understood in *Porphyromonas gingivalis* and much of the phylum *Bacteroidetes*. These Gram negative, anaerobic bacteria are integral parts of the human microbiome. Reactive nitrogen species can reach high levels in the oral cavity and the host immune system utilizes NO synthases as an antimicrobial. In order to inhabit the various parts of the body these microbes call home, they must have an efficient system in place to clear these toxic species. *P. gingivalis* is capable of withstanding the high concentrations of reactive nitrogen species and thus it is able to survive and grow in the oral cavity. It can also tolerate exposure to nitric oxide allowing it to survive the host immune response, which is elevated in the periodontal pockets during periodontitis. In *P. gingivalis*, Hcp is required for survival and bacterial growth in the presence of reactive nitrogen species. The FNR-like regulator, HcpR, activates the expression of Hcp in *P. gingivalis* in response to exposure to reactive nitrogen species. The exact mechanisms HcpR uses to modulate the expression of Hcp are not known. To efficiently regulate the nitrosative stress response, HcpR must effectively and efficiently bind the diatomic gas molecule, NO, and modulate the expression of its effector genes, which will clear the toxic species. In this study, we show that HcpR binds heme and in the presence of NO, the iron moiety is nitrosylated.

FNR-like transcription factors are found in many species of anaerobic bacteria and have been proven to play a role in the regulation of oxidative and nitrosative stress responses (although they are not limited to these functions). In the presence of oxides and N-oxides, they promote the expression of genes such as *nir, nor,* and *nos* which are responsible for detoxification and denitrification (Arai, Igarashi et al. 1995, Arai, Mizutani

et al. 2003). Bioinformatics studies revealed that HcpR shares a 69% sequence similarity to DNR, an FNR-like regulator found in *Pseudomonas aeruginosa*. Using DNR as a template, a working HcpR homology model was constructed. As most bacterial transcription factors (and all members of the FNR-like family), HcpR was modeled as a dimer.

Upon exposure to NO or nitrite, *hcp* is the most upregulated gene. The *hcp* gene encodes for a putative hydroxylamine reductase, although the gene products exact function(s) in *P. gingivalis* are still under much scrutiny. In other obligate and facultative anaerobes, Hcp has been shown to play an important role in NO and hydroxylamine reduction and detoxification (Rodionov, Dubchak et al. 2005, Chismon, Browning et al. 2010). Previous studies have shown that *hcp* is a required gene for growth of *P. gingivalis* in the oral cavity, infection of the periodontal pockets, and invasion of host epithelial cells.

Initial purifications of HcpR using the pET30 His-tag method yielded a pure, highly expressed, recombinant protein. However, initial characterization revealed HcpR was a tetramer in solution. The initial native gel (Fig. 12), high-performance liquid chromatography (HPLC), and SAXS experiments produced results indicating that HcpR was a 100 kDa tetramer. This initial finding was both shocking and confusing. The recombinant protein that is produced by the pET30a plasmid yields a product that has a rather large, N-terminal tag (approximately 8 kDa) with an enterokinase cleavage site. Attempts to remove the tag using enterokinase were unsuccessful, thus we turned to the Halo-tag method of purifying the protein. The Halo-tag purification yields a very pure protein very quickly, however it is not a viable purification method to purify large

amounts of the protein. The modified-pET21 vector removes the T7 tag that is expressed on the N-terminal of the recombinant protein and adds a TEV protease cleavage site between the C-terminus of the protein and the 6x His tag. The modified-pET21 vector allows for large scale purification of tag-less HcpR to be used in our assays.

As expected, HcpR is a dimer in solution after the removal of the affinity tag using either the Halo or pET21 recombinant proteins as confirmed by subsequent analytical ultracentrifugation and SAXS experiments. This puts HcpR in agreement with other members of the FNR-like family.

Binding of heme to the protein is a necessary step in the full activation of HcpR and is required for proper function of the protein. The exact mechanism by which HcpR binds heme is not known, however, it is possible HcpR is alone sufficient to bind heme. From our studies, it appears that HcpR does not bind heme efficiently under aerobic conditions. The TMBZ heme shift assay reveals that heme is binding to the protein, however, it is entirely possible that heme is binding nonspecifically. Heme is a very hydrophobic molecule and has a “sticky” nature to it at physiological pH, causing it to bind to places other than the heme binding domain. The fluorescence binding assay yields an extremely low affinity binding constant. This would require heme concentrations well above the physiological levels. It is possible that the drop in fluorescence is nonspecific binding of the heme, causing partial unfolding of the protein. This exposes the tryptophan residue to solvent, thus quenching the fluorescence. This is supported by the SAXS data. The Kratky plots of the heme samples indicate that there is partial unfolding of the protein. Furthermore, there is no Soret peak in the UV-

Vis scan when heme binding is tested under aerobic conditions. The Soret peak is characteristic of most heme proteins and appears in the 400 nm range. It is possible that the presence of oxygen in the sample inhibits the binding of heme through interaction with the heme.

A very strong Soret peak appears upon doing the experiment under anaerobic conditions. The anaerobic, resonance Raman spectrum also reveals the 4 vibrational modes that are common among heme proteins. These peaks do not arise from unbound, free heme in solution. Taken together, this indicates that aerobic conditions inhibit heme binding in some unknown way. It is possible that the free heme in solution is coordinating oxygen molecules between two heme molecules, thus inhibiting the binding of heme to the protein. By removing the competition from oxygen, this frees up heme to bind. Also, it is possible that the use of heme derived from hemin may be causing some unknown binding problems.

The oxidations state of the iron also appears to affect the Soret peak. Although the exact mechanism is not well understood, dithionite is used to oxidize ferrous iron to the ferric form. Addition of dithionite to the sample creates a shoulder on the Soret peak at approximately 350 nm, there is also a shift in the minor peak at the ~620 nm. The Soret peak arises from an electron dipole moment that allows a π to π* transition of the porphyrin ring, changing of the oxidation state of the iron changes the dipole moment and changes the energy of the peak (Shkirman, Solov'ev et al. 1999). We hypothesize that the addition of NO nitrosylates the iron, reducing Fe^{3+} and yielding Fe^{2+}, causing a conformational change and activation of the protein. Addition of NO appears to reduce

the ferric iron to the ferrous form as predicted. The spectrum reverts to the ferrous form: the shoulder at 350 nm is lost and the peak at ~620 nm shifts back to ~570 nm.

Binding of NO is also supported by Resonance Raman spectroscopy. The 1362 cm^{-1} peak is indicative of a high spin unbound form of the heme and the 1376 cm^{-1} peak is indicative of a low spin ligand-bound heme (this is a common theme among heme protein such as hemoglobin). The Raman spectrum of the un-nitrosylated, reduced sample appears to indicate the presence of a ferric, high spin heme. Upon addition of NO, there is a complete shift in the very large 1362 cm^{-1} peak to the 1372 cm^{-1}peak, indicating the presence of a low spin, ligand bound heme. It should be noted that in the sample without NO there appears to be a mixed population of heme. In the un-nitrosylated form of the protein, there is a smaller peak at 1376 cm^{-1} that can be seen in the polarized data that is overtaken by the much larger 1362 cm^{-1} peak. This could be due to a number of reasons: exposure to air can oxidize the reduced sample or the sample was never fully reduced by the dithionite.

The oxidation state of the heme may play a role in binding specificity for the protein. Oxygen and carbon monoxide cannot bind ferric heme; NO is the only diatomic gas molecule that is capable of binding to ferric heme. This is due the contraction of the d_{π} orbitals in Fe(III), which disallows the binding of O_2 or CO. However, the odd electron on NO can spontaneously transfer to Fe(III), producing a Fe(II)-NO^+ resonance structure (Soldatova, Ibrahim et al. 2010). The Fe(II)-NO^+ resonance structure can be reduced by OH^- in solution. The anaerobic nature inside *P. gingivalis* promotes a reduced environment inside the bacterium (there is a semi-reduced environment in most bacteria). It is believed the oxidative stress response in *P. gingivalis* uses other

mechanisms to promote expression of the necessary gene to clear the reactive oxygen species. HcpR's use of ferric heme discriminates the activation of the protein towards only activating in the presence of NO.

Although creating a crystal that yields a decent resolution has eluded us, it may be possible to obtain a decent resolution with the current crystal conditions if a large enough crystal can be grown. Diffraction from these crystals are better than those previously tested, if a bigger crystal can be obtained then a full x-ray data set with reasonable resolution is probable. The mosaicity is too high and a better cryo condition must be found: ethylene glycol, MPD, DMSO, and sucrose still have to be tested.

The SAXS scattering profile yields an *ab initio* model that is very alike in volume and shape to our homology model. With SAXS data, it is possible to insert inherent bias in the analysis of the data sets. The theoretical homology model scattering profiles generated matches our scattering profile, reinforcing our extrapolations made from the data in comparison to the homology model. These data indicate that the homology model may be used to solve the structure of the protein through molecular replacement.

The *hcp* promoter assay would be a valuable tool to analyze the biological significance of HcpR and probe the structure of HcpR for necessary components (such as residues vital for activation). However, using NO and nitrite, we saw no dose dependent change in the expression of the fluorescence reporter gene in the promoter studies. This is most likely due to an inefficiency of *E. coli* to express a gene under control of the *P. gingivalis* promoter. Phylogenetically speaking, *E. coli* and *P. gingivalis* are distant relatives, and the mechanisms and tools *E. coli* uses to express genes are different. The RNA polymerase of *P. gingivalis* is unrelated to the RNA polymerase of *E.*

coli (Klimpel, Clark 1990). Furthermore, *E. coli* primary sigma factor is considerably different than the primary sigma factor found in members of the phylum Bacteroidetes (Vingadassalom, Kolb et al. 2005). The FNR binding sites at *E. coli* promoters bear no resemblance to the HcpR binding site at the *hcp* promoter in *P. gingivalis* (Barnard, Green et al. 2003). The Bacteroidetes ribosomal binding site and mechanisms of translation are considerably different than those found in *E. coli* (Wegmann, Horn et al. 2013). It is also very likely that the interactions that HcpR uses to recruit RNA polymerase and up-regulate expression of *hcp* are very different than the mechanisms FNR uses in *E. coli*. Taken together, there is not a lot *E. coli* and *P. gingivalis* have in common in terms of gene expression. Although unfortunate for our immediate studies, this suggests that the mechanisms used by *P. gingivalis* are novel and are unlike those found in *E. coli*.

Although we focus on HcpR's regulation at the *hcp* promoter, it is possible and probable that HcpR regulates the expression of other genes necessary for detoxification and dentrification. We clarify one small aspect of *P. gingivalis*' response to reactive nitrogen species, however, as a whole the process remains poorly understood. Real-time PCR analysis and micro-array analysis reveal the modulation of a number of *P. gingivalis* genes when exposed to NO (Boutrin, Wang et al. 2012). Many of these genes are hypothetical, uncategorized, or unknown and could be directly involved in the stress response.

Conclusion

This work identifies important properties of HcpR, and how it regulates the stress response to NO in *P. gingivalis*. We show that HcpR is a transcription factor that exists as a dimer in solution and binds the heme cofactor. The properties and structure of HcpR is similar to those found in other members of the FNR-like family of transcription factors. The heme cofactor is a necessary component of the protein in its role as a sensor protein. Heme allows HcpR to recognize and specifically bind NO. Upon binding of NO, we show evidence that there is a switch in oxidation state of the iron. We hypothesize that NO binding leads to a conformational change in the structure of HcpR, activating the protein and allowing it to up-regulate expression at the *hcp* promoter.

Bibliography

ALDERTON, W.K., COOPER, C.E. and KNOWLES, R.G., 2001. Nitric oxide synthases: structure, function and inhibition. *The Biochemical journal,* **357**(Pt 3), pp. 593-615.

AMANO, A., NAKAGAWA, I., OKAHASHI, N. and HAMADA, N., 2004. Variations of Porphyromonas gingivalis fimbriae in relation to microbial pathogenesis. *Journal of periodontal research,* **39**(2), pp. 136-142.

ANDREW, C.R., GREEN, E.L., LAWSON, D.M. and EADY, R.R., 2001. Resonance Raman Studies of Cytochrome câ€˜ Support the Binding of NO and CO to Opposite Sides of the Heme:â€‰ Implications for Ligand Discrimination in Heme-Based Sensorsâ€ . *Biochemistry,* **40**(13), pp. 4115-4122.

ARAI, H., MIZUTANI, M. and IGARASHI, Y., 2003. Transcriptional regulation of the nos genes for nitrous oxide reductase in Pseudomonas aeruginosa. *Microbiology (Reading, England),* **149**(Pt 1), pp. 29-36.

ARAI, H., IGARASHI, Y. and KODAMA, T., 1995. Expression of the nir and nor genes for denitrification of Pseudomonas aeruginosa requires a novel CRP/FNR-related transcriptional regulator, DNR, in addition to ANR. *FEBS letters,* **371**(1), pp. 73-76.

BARNARD, A.M., GREEN, J. and BUSBY, S.J., 2003. Transcription regulation by tandem-bound FNR at Escherichia coli promoters. *Journal of Bacteriology,* **185**(20), pp. 5993-6004.

BECK, J., GARCIA, R., HEISS, G., VOKONAS, P.S. and OFFENBACHER, S., 1996. Periodontal disease and cardiovascular disease. *Journal of periodontology,* **67**(10 Suppl), pp. 1123-1137.

BELIAEV, A.S., THOMPSON, D.K., KHARE, T., LIM, H., BRANDT, C.C., LI, G., MURRAY, A.E., HEIDELBERG, J.F., GIOMETTI, C.S., YATES, J., NEALSON, K.H., TIEDJE, J.M. and ZHOU, J., 2002. Gene and Protein Expression Profiles ofShewanella oneidensisduring Anaerobic Growth with Different Electron Acceptors. *OMICS: A Journal of Integrative Biology,* **6**(1), pp. 39-60.

BELIBASAKIS, G.N., BOSTANCI, N., HASHIM, A., JOHANSSON, A., ADUSE-OPOKU, J., CURTIS, M.A. and HUGHES, F.J., 2007. Regulation of RANKL and OPG gene expression in human gingival fibroblasts and periodontal ligament cells by Porphyromonas gingivalis: a putative role of the Arg-gingipains. *Microbial pathogenesis,* **43**(1), pp. 46-53.

BOUTRIN, M.C., WANG, C., ARUNI, W., LI, X. and FLETCHER, H.M., 2012. Nitric oxide stress resistance in Porphyromonas gingivalis is mediated by a putative hydroxylamine reductase. *Journal of Bacteriology,* **194**(6), pp. 1582-1592.

BRYK, R., GRIFFIN, P. and NATHAN, C., 2000. Peroxynitrite reductase activity of bacterial peroxiredoxins. *Nature,* **407**(6801), pp. 211-215.

BUHLIN, K., MÄNTYLÄ, P., PAJU, S., PELTOLA, J.S., NIEMINEN, M.S., SINISALO, J. and PUSSINEN, P.J., 2011. Periodontitis is associated with angiographically verified coronary artery disease. *Journal of clinical periodontology,* **38**(11), pp. 1007-1014.

CADBY, I., BUSBY, S. and COLE, J., 2011. An HcpR homologue from Desulfovibrio desulfuricans and its possible role in nitrate reduction and nitrosative stress. *Biochem Soc Trans,* **39**(1), pp. 224-229.

CASTIGLIONE, N., RINALDO, S., GIARDINA, G. and CUTRUZZOLA, F., 2009. The transcription factor DNR from Pseudomonas aeruginosa specifically requires nitric oxide and haem for the activation of a target promoter in Escherichia coli. *Microbiology (Reading, England),* **155**(Pt 9), pp. 2838-2844.

CHISMON, D.L., BROWNING, D.F., FARRANT, G.K. and BUSBY, S.J.W., 2010. Unusual organization, complexity and redundancy at theEscherichia coli hcp-hcroperon promoter. *Biochemical Journal,* **430**(1), pp. 61-68.

D'AIUTO, F., PARKAR, M., NIBALI, L., SUVAN, J., LESSEM, J. and TONETTI, M.S., 2006. Periodontal infections cause changes in traditional and novel cardiovascular risk factors: Results from a randomized controlled clinical trial. *American Heart Journal,* **151**(5), pp. 977 <last_page> 984.

DARVEAU, R.P., TANNER, A. and PAGE, R.C., 1997. The microbial challenge in periodontitis. *Periodontology 2000,* **14**, pp. 12-32.

DUDZINSKI, D.M. and MICHEL, T., 2007. Life history of eNOS: partners and pathways. *Cardiovascular research,* **75**(2), pp. 247-260.

EKE, P.I., DYE, B.A., WEI, L., THORNTON-EVANS, G.O. and GENCO, R.J., 2012. Prevalence of Periodontitis in Adults in the United States: 2009 and 2010. *Journal of dental research,* **91**(10), pp. 914-920.

ENERSEN, M., NAKANO, K. and AMANO, A., 2013. Porphyromonas gingivalis fimbriae. *Journal of oral microbiology,* **5**, pp. 10.3402/jom.v5i0.20265. Print 2013.

FANG, F.C., 2004. Antimicrobial reactive oxygen and nitrogen species: concepts and controversies. *Nature reviews.Microbiology,* **2**(10), pp. 820-832.

GARDNER, A.M., HELMICK, R.A. and GARDNER, P.R., 2002. Flavorubredoxin, an inducible catalyst for nitric oxide reduction and detoxification in Escherichia coli. *The Journal of biological chemistry,* **277**(10), pp. 8172-8177.

GIARDINA, G., RINALDO, S., CASTIGLIONE, N., CARUSO, M. and CUTRUZZOLA, F., 2009. A dramatic conformational rearrangement is necessary for the activation of DNR from Pseudomonas aeruginosa. Crystal structure of wild-type DNR. *Proteins,* **77**(1), pp. 174-180.

GIBBONS, R.J. and HOUTE, J.V., 1975. Bacterial adherence in oral microbial ecology. *Annual Review of Microbiology,* **29**, pp. 19-44.

GRAVES, D.T. and COCHRAN, D., 2003. The contribution of interleukin-1 and tumor necrosis factor to periodontal tissue destruction. *Journal of periodontology,* **74**(3), pp. 391-401.

GRENIER, D., BERTRAND, J. and MAYRAND, D., 1995. Porphyromonas gingivalis outer membrane vesicles promote bacterial resistance to chlorhexidine. *Oral microbiology and immunology,* **10**(5), pp. 319-320.

HAJISHENGALLIS, G., DARVEAU, R.P. and CURTIS, M.A., 2012. The keystone-pathogen hypothesis. *Nature Reviews Microbiology,* **10**(10), pp. 717-725.

HAJISHENGALLIS, G., LIANG, S., PAYNE, M.A., HASHIM, A., JOTWANI, R., ESKAN, M.A., MCINTOSH, M.L., ALSAM, A., KIRKWOOD, K.L., LAMBRIS, J.D., DARVEAU, R.P. and CURTIS, M.A., 2011. Low-Abundance Biofilm Species Orchestrates Inflammatory Periodontal Disease through the Commensal Microbiota and Complement. *Cell Host & Microbe,* **10**(5), pp. 497-506.

HAMMES, W.P., 2012. Metabolism of nitrate in fermented meats: The characteristic feature of a specific group of fermented foods. *Food Microbiology,* **29**(2), pp. 151-156.

HASEGAWA, Y., MANS, J.J., MAO, S., LOPEZ, M.C., BAKER, H.V., HANDFIELD, M. and LAMONT, R.J., 2007. Gingival epithelial cell transcriptional responses to commensal and opportunistic oral microbial species. *Infection and immunity,* **75**(5), pp. 2540-2547.

HENRY, L.G., MCKENZIE, R.M., ROBLES, A. and FLETCHER, H.M., 2012. Oxidative stress resistance in Porphyromonas gingivalis. *Future microbiology,* **7**(4), pp. 497-512.

HILL, B.G., DRANKA, B.P., BAILEY, S.M., LANCASTER, J.R. and DARLEY-USMAR, V.M., 2010. What Part of NO Don't You Understand? Some Answers to the Cardinal Questions in Nitric Oxide Biology. *Journal of Biological Chemistry,* **285**(26), pp. 19699-19704.

HUFFMAN, J.L. and BRENNAN, R.G., 2002. Prokaryotic transcription regulators: more than just the helix-turn-helix motif. *Current opinion in structural biology,* **12**(1), pp. 98-106.

JONES, P., BINNS, D., CHANG, H.Y., FRASER, M., LI, W., MCANULLA, C., MCWILLIAM, H., MASLEN, J., MITCHELL, A., NUKA, G., PESSEAT, S., QUINN, A.F., SANGRADOR-VEGAS, A., SCHEREMETJEW, M., YONG, S.Y., LOPEZ, R. and HUNTER, S., 2014. InterProScan 5: genome-scale protein function classification. *Bioinformatics (Oxford, England),* .

KELLEY, L.A. and STERNBERG, M.J.E., 2009. Protein structure prediction on the Web: a case study using the Phyre server. *Nature Protocols,* **4**(3), pp. 363 <last_page> 371.

KLEIN, R.S., HARRIS, C.A., SMALL, C.B., MOLL, B., LESSER, M. and FRIEDLAND, G.H., 1984. Oral Candidiasis in High-Risk Patients as the Initial Manifestation of the Acquired Immunodeficiency Syndrome. *New England Journal of Medicine,* **311**(6), pp. 354 <last_page> 358.

KLIMPEL, K.W. and CLARK, V.L., 1990. The RNA polymerases of Porphyromonas gingivalis and Fusobacterium nucleatum are unrelated to the RNA polymerase of Escherichia coli. *Journal of dental research,* **69**(9), pp. 1567-1572.

KONE, B.C., KUNCEWICZ, T., ZHANG, W. and YU, Z.Y., 2003. Protein interactions with nitric oxide synthases: controlling the right time, the right place, and the right amount of nitric oxide. *American journal of physiology.Renal physiology,* **285**(2), pp. F178-90.

KOPPENOL, W.H., 2001. 100 Years of Peroxynitrite Chemistry and 11 Years of Peroxynitrite Biochemistry. *Redox report : communications in free radical research,* **6**(6), pp. 339-341.

KRONCKE, K.D., FEHSEL, K. and KOLB-BACHOFEN, V., 1997. Nitric oxide: cytotoxicity versus cytoprotection--how, why, when, and where? *Nitric oxide : biology and chemistry / official journal of the Nitric Oxide Society,* **1**(2), pp. 107-120.

LAMONT, R.J., CHAN, A., BELTON, C.M., IZUTSU, K.T., VASEL, D. and WEINBERG, A., 1995. Porphyromonas gingivalis invasion of gingival epithelial cells. *Infection and immunity,* **63**(10), pp. 3878-3885.

LAMONT, R.J. and YILMAZ, O., 2002. In or out: the invasiveness of oral bacteria. *Periodontology 2000,* **30**(1), pp. 61-69.

LANCASTER, J.R.,Jr, 1997. A tutorial on the diffusibility and reactivity of free nitric oxide. *Nitric oxide : biology and chemistry / official journal of the Nitric Oxide Society,* **1**(1), pp. 18-30.

LATCHMAN, D.S., 1997. Transcription factors: An overview. *The international journal of biochemistry & cell biology,* **29**(12), pp. 1305-1312.

LEON, R., SILVA, N., OVALLE, A., CHAPARRO, A., AHUMADA, A., GAJARDO, M., MARTINEZ, M. and GAMONAL, J., 2007. Detection of Porphyromonas gingivalis in the amniotic fluid in pregnant women with a diagnosis of threatened premature labor. *Journal of periodontology,* **78**(7), pp. 1249-1255.

LEWIS, J.P., 2010. Metal uptake in host-pathogen interactions: role of iron in Porphyromonas gingivalis interactions with host organisms. *Periodontology 2000,* **52**(1), pp. 94-116.

LEWIS, J.P., YANAMANDRA, S.S. and ANAYA-BERGMAN, C., 2012. HcpR of Porphyromonas gingivalis is required for growth under nitrosative stress and survival within host cells. *Infection and immunity,* **80**(9), pp. 3319-3331.

LIEBL, U., LAMBRY, J. and VOS, M.H., 2013. Primary processes in heme-based sensor proteins. *Biochimica et Biophysica Acta (BBA) - Proteins and Proteomics,* **1834**(9), pp. 1684-1692.

LUNDBERG, J.O., WEITZBERG, E., COLE, J.A. and BENJAMIN, N., 2004. Nitrate, bacteria and human health. *Nature reviews.Microbiology,* **2**(7), pp. 593-602.

OGRENDIK, M., KOKINO, S., OZDEMIR, F., BIRD, P.S. and HAMLET, S., 2005. Serum antibodies to oral anaerobic bacteria in patients with rheumatoid arthritis. *MedGenMed : Medscape general medicine,* **7**(2), pp. 2.

OKAMOTO, K., KADOWAKI, T., NAKAYAMA, K. and YAMAMOTO, K., 1996. Cloning and sequencing of the gene encoding a novel lysine-specific cysteine proteinase (Lys-gingipain) in Porphyromonas gingivalis: structural relationship with the arginine-specific cysteine proteinase (Arg-gingipain). *Journal of Biochemistry,* **120**(2), pp. 398-406.

OKAMOTO, K., MISUMI, Y., KADOWAKI, T., YONEDA, M., YAMAMOTO, K. and IKEHARA, Y., 1995. Structural characterization of argingipain, a novel arginine-specific cysteine proteinase as a major periodontal pathogenic factor from Porphyromonas gingivalis. *Archives of Biochemistry and Biophysics,* **316**(2), pp. 917-925.

PABO, C.O. and SAUER, R.T., 1992. Transcription factors: structural families and principles of DNA recognition. *Annual Review of Biochemistry,* **61**, pp. 1053-1095.

PALMERINI, C.A., PALOMBARI, R., PERITO, S. and ARIENTI, G., 2003. NO Synthesis in Human Saliva. *Free radical research,* **37**(1), pp. 29-31.

PARK, Y., SIMIONATO, M.R., SEKIYA, K., MURAKAMI, Y., JAMES, D., CHEN, W., HACKETT, M., YOSHIMURA, F., DEMUTH, D.R. and LAMONT, R.J., 2005. Short fimbriae of Porphyromonas gingivalis and their role in coadhesion with Streptococcus gordonii. *Infection and immunity,* **73**(7), pp. 3983-3989.

PATHANIA, R., NAVANI, N.K., GARDNER, A.M., GARDNER, P.R. and DIKSHIT, K.L., 2002. Nitric oxide scavenging and detoxification by the Mycobacterium tuberculosis haemoglobin, HbN in Escherichia coli. *Molecular microbiology,* **45**(5), pp. 1303-1314.

PETTERSEN, E.F., GODDARD, T.D., HUANG, C.C., COUCH, G.S., GREENBLATT, D.M., MENG, E.C. and FERRIN, T.E., 2004. UCSF Chimera--a visualization system for exploratory research and analysis. *Journal of computational chemistry,* **25**(13), pp. 1605-1612.

PTASHNE, M. and GANN, A., 1997. Transcriptional activation by recruitment. *Nature,* **386**(6625), pp. 569-577.

RODIONOV, D.A., DUBCHAK, I., ARKIN, A., ALM, E. and GELFAND, M.S., 2004. Reconstruction of regulatory and metabolic pathways in metal-reducing delta-proteobacteria. *Genome biology,* **5**(11), pp. R90.

RODIONOV, D.A., DUBCHAK, I.L., ARKIN, A.P., ALM, E.J. and GELFAND, M.S., 2005. Dissimilatory metabolism of nitrogen oxides in bacteria: comparative reconstruction of transcriptional networks. *PLoS computational biology,* **1**(5), pp. e55.

SAGLIE, R., NEWMAN, M.G., CARRANZA, F.A.,Jr and PATTISON, G.L., 1982. Bacterial invasion of gingiva in advanced periodontitis in humans. *Journal of periodontology,* **53**(4), pp. 217-222.

SAVAGE, A., EATON, K.A., MOLES, D.R. and NEEDLEMAN, I., 2009. A systematic review of definitions of periodontitis and methods that have been used to identify this disease. *Journal of clinical periodontology,* **36**(6), pp. 458-467.

SCHIFFERLE, R.E., SHOSTAD, S.A., BAYERS-THERING, M.T., DYER, D.W. and NEIDERS, M.E., 1996. Effect of protoporphyrin IX limitation on porphyromonas gingivalis. *Journal of endodontics,* **22**(7), pp. 352-355.

SCHULTZ, S.C., SHIELDS, G.C. and STEITZ, T.A., 1991. Crystal structure of a CAP-DNA complex: the DNA is bent by 90 degrees. *Science (New York, N.Y.),* **253**(5023), pp. 1001-1007.

SHKIRMAN, S.F., SOLOV'EV, K.N., KACHURA, T.F., ARABEI, S.A. and SKAKOVSKII, E.D., 1999. Interpretation of the soret band of porphyrins based on the polarization spectrum of N-methyltetraphenylporphin fluorescence. *Journal of Applied Spectroscopy,* **66**(1), pp. 68-75.

SLOTS, J., BRAGD, L., WIKSTROM, M. and DAHLEN, G., 1986. The occurrence of Actinobacillus actinomycetemcomitans, Bacteroides gingivalis and Bacteroides intermedius in destructive periodontal disease in adults. *Journal of clinical periodontology,* **13**(6), pp. 570-577.

SOLDATOVA, A.V., IBRAHIM, M., OLSON, J.S., CZERNUSZEWICZ, R.S. and SPIRO, T.G., 2010. New Light on NO Bonding in Fe(III) Heme Proteins from Resonance Raman Spectroscopy and DFT Modeling. *Journal of the American Chemical Society,* **132**(13), pp. 4614-4625.

SPIRO, S., 2006. Nitric oxide-sensing mechanisms in Escherichia coli. *Biochemical Society transactions,* **34**(Pt 1), pp. 200-202.

SPIRO, S., 1994. The FNR family of transcriptional regulators. *Antonie van Leeuwenhoek,* **66**(1-3), pp. 23-36.

SPIRO, T.G., SOLDATOVA, A.V. and BALAKRISHNAN, G., 2013. CO, NO and O as Vibrational Probes of Heme Protein Interactions. *Coordination Chemistry Reviews,* **257**(2), pp. 511-527.

SPIRO, T.G. and SOLDATOVA, A.V., 2012. Ambidentate H-bonding of NO and O2 in heme proteins. *Journal of inorganic biochemistry,* **115**, pp. 204-210.

SPIRO, T.G. and STREKAS, T.C., 1974. Resonance Raman spectra of heme proteins. Effects of oxidation and spin state. *Journal of the American Chemical Society,* **96**(2), pp. 338 <last_page> 345.

TOMITA, T., HIROTA, S., OGURA, T., OLSON, J.S. and KITAGAWA, T., 1999. Resonance Raman Investigation of Fe-N-O Structure of Nitrosylheme in Myoglobin and Its Mutants. *The Journal of Physical Chemistry B,* **103**(33), pp. 7044-7054.

VAN DEN BERG, W.A.M., HAGEN, W.R. and VAN DONGEN, W.M.A.M., 2000. The hybrid-cluster protein ('prismane protein') from Escherichia coli. *European Journal of Biochemistry,* **267**(3), pp. 666-676.

VINGADASSALOM, D., KOLB, A., MAYER, C., RYBKINE, T., COLLATZ, E. and PODGLAJEN, I., 2005. An unusual primary sigma factor in the Bacteroidetes phylum. *Molecular microbiology,* **56**(4), pp. 888-902.

WANDERSMAN, C. and STOJILJKOVIC, I., 2000. Bacterial heme sources: the role of heme, hemoprotein receptors and hemophores. *Current opinion in microbiology,* **3**(2), pp. 215-220.

WEGMANN, U., HORN, N. and CARDING, S.R., 2013. Defining the bacteroides ribosomal binding site. *Applied and Environmental Microbiology,* **79**(6), pp. 1980-1989.

YILMAZ, O., WATANABE, K. and LAMONT, R.J., 2002. Involvement of integrins in fimbriae-mediated binding and invasion by Porphyromonas gingivalis. *Cellular microbiology,* **4**(5), pp. 305-314.

ZHENG, M., 1998. Activation of the OxyR Transcription Factor by Reversible Disulfide Bond Formation. *Science,* **279**(5357), pp. 1718-1722.

ZHENG, M. and STORZ, G., 2000. Redox sensing by prokaryotic transcription factors. *Biochemical pharmacology,* **59**(1), pp. 1-6.